



## City Research Online

### City, University of London Institutional Repository

---

**Citation:** Najibi, F., Apostolopoulou, D. & Alonso, E. (2021). TSO-DSO Coordination Schemes to Facilitate Distributed Resources Integration. *Sustainability*, 13(14), 7832. doi: 10.3390/su13147832

This is the accepted version of the paper.

This version of the publication may differ from the final published version.

---

**Permanent repository link:** <https://openaccess.city.ac.uk/id/eprint/26381/>

**Link to published version:** <https://doi.org/10.3390/su13147832>

**Copyright:** City Research Online aims to make research outputs of City, University of London available to a wider audience. Copyright and Moral Rights remain with the author(s) and/or copyright holders. URLs from City Research Online may be freely distributed and linked to.

**Reuse:** Copies of full items can be used for personal research or study, educational, or not-for-profit purposes without prior permission or charge. Provided that the authors, title and full bibliographic details are credited, a hyperlink and/or URL is given for the original metadata page and the content is not changed in any way.

---

---

---

City Research Online:

<http://openaccess.city.ac.uk/>

[publications@city.ac.uk](mailto:publications@city.ac.uk)

---

# TSO-DSO Coordination Schemes to Facilitate Distributed Resources Integration

Fatemeh Najibi <sup>1</sup> , Dimitra Apostolopoulou <sup>2</sup> and Eduardo Alonso <sup>1,\*</sup>

<sup>1</sup> Artificial Intelligence Research Centre, Department of Computer Science, City, University of London, London, UK EC1V 0HB; Fatemeh.najibi@city.ac.uk, E.Alonso@city.ac.uk

<sup>2</sup> Department of Electrical and Electronic Engineering at City, University of London, London, UK EC1V 0HB; Dimitra.Apostolopoulou@city.ac.uk

\* Correspondence: Fatemeh.Najibi@city.ac.uk

**Abstract:** The incorporation of renewable energy into power systems poses serious challenges to the transmission and distribution power system operators (TSOs and DSOs). To fully leverage these resources there is a need for a new market design with improved coordination between TSOs and DSOs. In this paper we propose two coordination schemes between TSOs and DSOs: one centralised and another decentralised that facilitate the integration of distributed based generation; minimise operational cost; relieve congestion; and promote a sustainable system. **In order to achieve this**, we approximate the power equations with linearised equations so that the resulting optimal power flows (OPFs) in both the TSO and DSO become convex optimisation problems. In the resulting decentralised scheme, the TSO and DSO collaborate to optimally allocate all resources in the system. In particular, we propose an iterative bi-level optimisation technique where the upper level is the TSO that solves its own OPF and determines the locational marginal prices at substations. We demonstrate numerically that the algorithm converges to a near optimal solution. We study the interaction of TSOs and DSOs and the existence of any conflicting objectives with the centralised scheme. More specifically, we approximate the Pareto front of the multi-objective optimal power flow problem where the entire system, i.e., transmission and distribution systems, is modelled. The proposed ideas are illustrated through a five bus transmission system connected with distribution systems, represented by the IEEE 33 and 69 bus feeders.

**Keywords:** TSO-DSO coordination, Pareto front, Bi-level optimisation, Optimal power flow

**Citation:** Najibi, F.; Apostolopoulou, D.; Alonso, E. Title. *Journal Not Specified* **2021**, *1*, 0. <https://doi.org/>

Received:  
Accepted:  
Published:

**Publisher's Note:** MDPI stays neutral with regard to jurisdictional claims in published maps and institutional affiliations.

**Copyright:** © 2021 by the authors. Submitted to *Journal Not Specified* for possible open access publication under the terms and conditions of the Creative Commons Attribution (CC BY) license (<https://creativecommons.org/licenses/by/4.0/>).

## 1. Introduction

In recent years, power systems have undergone critical changes as a result of the penetration of renewable energy. In turn, the incorporation of renewable energy into power systems poses serious challenges to transmission and distribution system operators (TSOs and DSOs). The transition to carbon-free power system is welcome, however concerns about the quality, voltage and frequency of such systems have been raised [1]. The main objective is to be able to use renewable energy sources (RESs) whereas guaranteeing efficient congestion management, reduction in operational costs, and increased flexibility while using local energy resources [2], [3], [4]. Working in this direction, governments have introduced incentives through policies that support the integration of RESs and encourage the collaboration and coordination of operators to maintain reliable and cost efficient power systems [5], [6]. **For instance, in [7] a hierarchical economic dispatch model was proposed to control the congestion in a power network and provide a unified bid function to network operators. In [8], the authors addressed issues about the intermittent nature of non-dispatchable resources which requires the network operators cooperate on new regulations, network designs, and congestion management solutions.**

Ancillary services are an example of the need of coordination between TSOs and DSOs [9]. More specifically, RESs can provide distribution systems with ancillary

38 services such as spinning reserves, voltage support and real-time frequency control.  
39 Currently, such services are commonly priced, and cleared in the wholesale markets.  
40 However, to fully leverage such services from these resources it is paramount to create  
41 a new market design where new technologies such as microgrids become smoothly  
42 integrated into power systems [10], [11]. Existing centralised power market models  
43 lack appropriate mechanisms to insert more environmentally friendly resources into  
44 distributed grids. For instance, the TSO solves its own optimal power flow (OPF) and  
45 determines the locational marginal prices (LMPs) at the substations. Next, the DSOs  
46 dispatch distributed generation (DG) by optimising cost and considering the LMP at the  
47 substation as a fixed parameter. To facilitate the integration of RESs into power systems  
48 the interaction between TSOs and DSOs, that are responsible for balancing the demand  
49 and supply, could be further improved (see, e.g., [12],[13]).

### 50 1.1. Literature Review

51 Research has been focused in proposing methods that increase the level of coordi-  
52 nation between TSOs and DSOs. These vary from centralised to totally decentralised  
53 methodologies. In centralised schemes the TSO is responsible for satisfying the system  
54 demand in both the transmission and distribution systems with the use of generators  
55 at both levels. In a more common market model on the other hand, each operator is  
56 responsible for its own operation cost minimisation taking into account the RESs con-  
57 nected to each system respectively [14]. Such models are referred to as decentralised  
58 schemes where the TSO and DSO collaborate [15]. More specifically, in decentralised  
59 schemes DSOs and TSOs need to agree on the point of common coupling (PCC) power  
60 flow interchange. The DSO operates its local system considering the bid that the TSO  
61 provides to supply energy to the distribution system at the PCC; this is usually the LMP  
62 at the PCC. Before solving the DSO OPF, the TSO solves its own OPF representing the  
63 entire distribution system by its net load. Therefore, the DSO can operate its system  
64 with the knowledge of the supply function for the real power, i.e., the bid function, from  
65 the TSO. After the DSO solves the OPF considering the local constraints, the DSO can  
66 again participate in the TSO market and receive the payment for its energy supply sent  
67 back to the transmission system [16]. Decentralised TSO-DSO coordination approaches  
68 are categorised as hierarchical or distributed [17]. In hierarchical TSO-DSO coordina-  
69 tion schemes, the interaction between distributed resources in the distribution (lower  
70 level) system and the transmission (upper level) power system is like a leader-follower  
71 type, where the leader has fixed decision variables and leads the followers in making  
72 decisions [18]. In distributed TSO-DSO, all local RESs connected to the market commu-  
73 nication graph can potentially be selected to meet the load. A detailed representation  
74 of the physical distribution system at a nodal basis as well as its market structure is  
75 necessary [19].

76 Several coordination schemes that can precisely model the system taking into ac-  
77 count nonlinear bi-directional AC power flow constraints present in transmission and  
78 distribution systems have been recently proposed. In [20], the authors propose five co-  
79 ordination schemes to evaluate the recent proposals of the SmartNet project consortium.  
80 In order to do so, they model the optimisation problem considering the AC load flow  
81 and the topology of the grid in each scheme. The main objective of this work was to  
82 quantify the proximity of the optimal solution to a physically compatible solution in  
83 different coordination schemes. In [21], the study aims at minimising the deviation from  
84 the real-time dispatch, and maximising the share contribution of renewable energy while  
85 addressing uncertainty using Dynamic AC Optimal Power Flow. In [22], distribution lo-  
86 cational marginal pricing is designed through quadratic programming. The case studies  
87 include a high number of electric vehicles and heat pumps to address issues associated  
88 with these resources in the distribution system. In [23], the authors summarise the main  
89 challenges proposed in the SmartNet project in three different countries (Denmark, Italy,

90 and Spain) by providing techno-economic analysis on various coordination schemes in  
91 2030 scenarios.

92 Alternative approaches are based on approximations of the AC power flow and  
93 represent the distribution and transmission systems with linearised power equations to  
94 overcome the challenges associated with nonlinearities (see, e.g., [24]). Approximations  
95 of AC power flow have been used in various problems in power systems that can also  
96 be applied in this particular setting. For instance, to control the reactive power at every  
97 bus, a method that approximates the distribution network into a linear distribution load  
98 flow was proposed in [25]. The results show that by linearising the load flow, the error  
99 on the voltage mismatch error is minimised. The authors in [26] address the power  
100 loss optimisation in smart power distribution by linearising the distribution power  
101 flow. This work demonstrates that the results of quadratic programming are better than  
102 conventional power flow in both robustness and computational complexity. In [27], a  
103 linear optimal load flow has been introduced using quadratic programming to cope with  
104 the increase in the number of DC microgrids.

105 How the network is represented is one of the main aspects to consider in TSO-  
106 DSO coordination. For instance, as the integration of RESs affects the voltage levels  
107 and the line thermal limits, network constraints need to be considered to ensure that  
108 these resources do not adversely disturb the power system operations [28]. In [29] the  
109 authors propose a coordination scheme which does not explicitly represent the grid  
110 topology but incorporates some information concerning, e.g., bus voltages. In [30], three  
111 market designs are proposed to mitigate coordination between the TSO and the DSO  
112 that provide a flexible, competitive market design for retailers. In the model, the main  
113 focus is on the market rather than on the operation and topology of the grid. A control  
114 framework that provides the DSO with information on the contribution of each smart  
115 home, the unbalanced power flow and network voltage constraints is given in [31]. In  
116 this way DG participates in the electricity market while ensuring that the upstream  
117 constraints are satisfied. In [13], three TSO-DSO coordination models are discussed.  
118 First, a TSO-managed model is presented, where the TSO is responsible for the optimal  
119 operation of the system by considering DG and transmission system constraints. Next,  
120 a TSO-DSO hybrid-managed model is introduced, where the TSO operates the system  
121 considering the transmission network constraints and the DG that submits bids to  
122 demonstrate its willingness to participate in the market. Last, a DSO-managed model  
123 is mentioned where the DSO is responsible for operating its own system taking into  
124 account the distributed energy sources and sending back the outcomes to the TSO [20].  
125 Centralised TSO-managed schemes make the coordination model simpler to implement  
126 (see, e.g., [1]). By using a centralised scheme, we utilise the traditional SCADA system  
127 to monitor, measure and collect the data from different assets of the grid [32]. However,  
128 they might fail to fully utilise DG resources at the distribution system since the DSO  
129 has less visibility of their usage. TSO-DSO hybrid systems are an improvement of the  
130 latter since DG resources indicate by their bids to the TSO and DSO their willingness to  
131 participate; and both operators based on their priorities can decide whether they accept  
132 the offer or not [33], [34]. A DSO-managed scheme has the potential to reach to the  
133 highest level of efficient use of distributed resources. However, it incorporates the risk  
134 that there might be a conflict between the TSO and DSO requirements and needs; thus  
135 making a real-time exchange of information between both operators necessary to ensure  
136 a reliable operation.

### 137 1.2. Gap Analysis

138 Notwithstanding the merits of the above-mentioned solutions, there are still gaps to  
139 assist operators with practical solutions to smoothly adapt to the large-scale integration  
140 of renewable energy resources and to reliably transition into the carbon-free power  
141 systems. The aforementioned centralised schemes face a variety of regulatory challenges  
142 that make their actual implementation difficult. However, centralised schemes can still

143 be used to provide insights into the desired coordination between TSOs and DSOs. As  
144 such, in practice, decentralised schemes need to be further investigated. These schemes  
145 need to respect the privacy concerns of the entities involved, be computationally effi-  
146 cient, depend on realistic communication infrastructure, achieve an optimal with some  
147 objective outcome, relieve congestion, and facilitate the integration of renewable-based  
148 generation. As discussed in the previous section, the methods present in the literature  
149 fail to meet at least one of the above-mentioned points.

### 150 151 *1.3. Contributions*

152 In this paper, we add to existing methodologies by (i) constructing a centralised  
153 TSO-DSO framework which is used to quantify the operators' conflicting objectives and  
154 provide appropriate incentives for their coordination; and based on this analysis by (ii)  
155 proposing a decentralised TSO-DSO scheme that reaches a near-least cost solution by  
156 respecting the privacy concerns of TSOs, DSOs; is computationally efficient; relieves  
157 congestion; and increases the level of DG resources' integration.

158 More specifically, we propose a linear transmission-distribution system coordi-  
159 nation framework considering large-scale integration of distributed resources, e.g.,  
160 photovoltaic (PV) and storage. More specifically, we approximate the power equations  
161 with linearised equations so that the resulting optimal power flows performed by both  
162 the TSO and DSO are convex optimisation programmes (see, e.g., [24], [25]). Next, we  
163 propose two different coordination schemes, decentralised and centralised. In the decen-  
164 tralised scheme, the TSO and the DSO collaborate to allocate all resources in the system  
165 optimally. In particular, we develop an iterative bi-level optimisation technique where  
166 the upper level is the TSO. The TSO solves its own OPF and determines the LMPs at sub-  
167 stations. The LMPs are passed on to the lower level, a collection of DSOs, each of which  
168 solves its own OPF. The new demand of the distribution system is aggregated at the  
169 substation levels and sent back to the TSO. We iterate between the two levels until some  
170 stopping criterion, e.g., that the infinity norm of the vector containing the differences of  
171 LMPs at current and previous iterations does not change by some tolerance is met. We  
172 demonstrate numerically that this process converges to a point near the optimal solution.  
173 Moreover, in the numerical results' section, it is shown that the proposed decentralised  
174 scheme provides a balance between the TSO and DSO objective in terms of cost. It is  
175 worthy to note that the only information used in the iterative decentralised scheme is the  
176 customers' net load at the PCC; thus, there is no issue associated with privacy concerns  
177 of individual entities. In the proposed centralised scheme, the transmission system acts  
178 as the entire system operator and has all the necessary information about the distribution  
179 system. In such a case, the objective function consists of the distribution system voltage  
180 deviation from reference, the distributed resources cost, and the transmission system  
181 operating cost, aggregated as one objective with some weighting coefficients. We modify  
182 the weighting coefficients to approximate the Pareto front of the TSO and DSO objectives  
183 and study their interaction. In particular, we quantify the conflicting objectives of TSOs  
184 and DSOs, which DSOs may use to submit bids to the TSO or by the TSO to incentivise  
185 DSOs to provide their services appropriately. The proposed framework is validated by  
186 constructing a transmission distribution system using the 33 and 69 IEEE distribution  
187 feeders and a five node transmission system.

188 The remainder of the paper is organised as follows. In Section 2 we model the  
189 augmented DC OPF for the transmission system and a linear OPF for the distribution  
190 system. In Section 3, we formulate the proposed decentralised and centralised schemes.  
191 In Section 4, we illustrate the proposed framework through the constructed transmission-  
192 distribution system. In Section 5, we summarise the results and make some concluding  
193 remarks.

194

## 195 2. Optimal Power Flow Formulation

196 In this section, we formulate the linearized OPF models for transmission and  
 197 distribution systems. More specifically, we formulate the augmented DC OPF for the  
 198 transmission system by defining its objective and constraints. Next, we present the  
 199 linearized model for the network representation of the distribution system along with  
 200 other constraints and determine the objective of the DSO; these are used as input to the  
 201 DSO OPF.

### 202 2.1. Transmission level

203 The AC OPF at the transmission level is a nonlinear non-convex problem since it  
 204 has nonlinear equality constraints, e.g., the power balance. By using a DC formulation  
 205 of the power flow we obtain a convex problem which is known as the DC OPF. The  
 206 objective function at the transmission DC OPF usually comprises of the generators' cost.  
 207 In this paper, we augment the objective function with a soft penalty function on the  
 208 sum of the squared voltage angle differences, as suggested in [24]. This augmentation  
 209 has both physical and mathematic benefits. From a physical perspective, it provides  
 210 a way to conduct sensitivity experiments on the size of the voltage angle differences  
 211 that could be informative for estimating the size and pattern of AC-DC approximation  
 212 errors. From a mathematical perspective, the augmentation could help to improve the  
 213 numerical stability and convergence properties of any applied solution method. The  
 214 resulting augmented DCOPF is a strictly convex quadratic problem which can be solved  
 215 through quadratic programming. The constraints of the OPF refer to the nodal power  
 216 balance whose dual variables are the LMPs, the line flow limits, and the generation  
 217 limits.

218 We consider a time period of interest  $\mathcal{T} = \{1, \dots, T\}$  with time increments denoted  
 219 by  $\Delta t$  and a power system consisting of the set of  $K$  nodes  $\mathcal{K} = \{1, \dots, K\}$ , with the  
 220 slack bus at node 1. We denote the set of  $I$  generators by  $\mathcal{I} = \{1, \dots, I\}$ , the set of  $J$  loads  
 221 by  $\mathcal{J} = \{1, \dots, J\}$ , the set of generators connected to bus  $k$  by  $\mathcal{I}_k$ , i.e.,  $\mathcal{I} = \cup_{k \in \mathcal{K}} \mathcal{I}_k$ ;  
 222 the set of loads connected to bus  $k$  by  $\mathcal{J}_k$ , i.e.,  $\mathcal{J} = \cup_{k \in \mathcal{K}} \mathcal{J}_k$ ; and the set of  $L$  lines by  
 223  $\mathcal{L} = \{\ell_1, \dots, \ell_L\}$ . Each line is denoted by the ordered pair  $\ell = (n, m)$  where  $n$  is the *from*  
 224 node, and  $m$  is the *to* node with  $n, m \in \mathcal{K}$ , with the real power flow  $f_\ell \geq 0$  whenever  
 225 the flow is from  $n$  to  $m$  and  $f_\ell < 0$  otherwise. We assume that each bus is connected to at  
 226 least one other bus. We consider a lossless network with the diagonal branch susceptance  
 227 matrix  $B_d \in \mathbb{R}^{L \times L}$ . Let  $A \in \mathbb{R}^{L \times K}$  be the reduced branch-to-node incidence matrix for the  
 228 subset of nodes  $\mathcal{K} / \{1\}$  and  $B \in \mathbb{R}^{K \times K}$  be the corresponding nodal susceptance matrix.  
 229 We assume that the network contains no phase shifting devices and so  $B^\top = B$ . We  
 230 denote the slack bus nodal susceptance vector by  $b_1 = [b_{11}, \dots, b_{1K}]^\top$ , with  $b_1 + B \mathbb{1}^K = 0$ ,  
 231 where  $\mathbb{1}^K$  is the unit  $K$ -dimensional vector. We denote by  $P_{G_i}$  the power injection of  
 232 generator  $i \in \mathcal{I}$ ; by  $P_{L_j}$  the power withdrawal at load  $j \in \mathcal{J}$ ; and by  $\theta_k$  the angle at  
 233 node  $k$ . Since node 1 is the slack bus  $\theta_1 = 0$ .

The mathematical formulation of the augmented DC OPF at the transmission level  
 at hour  $t \in \mathcal{T}$  is presented as follows:

$$\begin{aligned}
 & \min_{P_{G_i}(t), i \in \mathcal{I}, \theta_k(t), k \in \mathcal{K}} \sum_{i \in \mathcal{I}} c_i(t) + \pi \sum_{\ell=(m,n) \in \mathcal{L}} (\theta_n(t) - \theta_m(t))^2 \\
 & \text{subject to } \sum_{i \in \mathcal{I}_k} P_{G_i}(t) - \sum_{\ell \in \mathcal{L}} B_{d_\ell} A \theta(t) = \sum_{j \in \mathcal{J}_k} P_{L_j}(t), k \in \mathcal{K}, \longleftrightarrow \lambda_k(t), \\
 & f^m \leq f(t) = B_d A \theta(t) \leq f^M, \\
 & P_G^m \leq P_G(t) \leq P_G^M, \tag{1}
 \end{aligned}$$

234 where  $B_{d_\ell}$  is the  $\ell^{\text{th}}$  row of the  $B_d$  matrix;  $f^M$  and  $f^m$  are the values of the maximum real  
 235 power flow allowed through the lines in  $\mathcal{L}$  in the same direction and in the opposite  
 236 direction of line  $\ell$  respectively and  $P_G^m$  ( $P_G^M$ ) is the vector of lower (upper) generation  
 237 limits. Usually, the cost of generator  $i \in \mathcal{I}$  is a quadratic function in the form of

238  $c_i(t) = \alpha_i P_{G_i}(t) + \beta_i P_{G_i}^2(t) + \gamma_i$ . The LMPs are the dual variables of the nodal power  
 239 balance denoted by  $\lambda(t) = [\lambda_1(t), \dots, \lambda_K(t)]^\top$ .

## 240 2.2. Distribution Level

241 We assume a radial distribution feeder with a set of  $N$  buses denoted by  $\mathcal{N}$  and a  
 242 set of  $N - 1$  lines denoted by  $\mathcal{L}'$ . Bus 1 denotes the PCC with the TSO and is considered  
 243 to be the slack bus. For each bus  $i$ ,  $V_i$  stands for the bus voltage magnitude while  $p_i$  and  
 244  $q_i$  represent the injected active and reactive power, respectively. For each line segment  
 245 in  $\mathcal{L}'$  that connects bus  $i$  to bus  $j$ ,  $r_{ij}$  and  $x_{ij}$  stand for its resistance and reactance, and  
 246  $P_{ij}$  and  $Q_{ij}$  for the real and reactive power from bus  $i$  to  $j$  respectively. In addition, the  
 247 set  $\mathcal{N}_j \subset \mathcal{N}$  denotes bus  $j$ 's neighbouring buses, which are further downstream. The  
 248 linear equations that model the distribution feeder for each line  $(i, j)$  are as follows (see,  
 249 e.g., [25]):

$$P_{ij} - \sum_{k \in \mathcal{N}_j} P_{jk} = -p_i + r_{ij} \frac{P_{ij}^2 + Q_{ij}^2}{V_i^2}, \quad (2)$$

$$Q_{ij} - \sum_{k \in \mathcal{N}_j} Q_{jk} = -q_i + r_{ij} \frac{P_{ij}^2 + Q_{ij}^2}{V_i^2}, \quad (3)$$

$$V_i^2 - V_j^2 = 2(r_{ij}P_{ij} + x_{ij}Q_{ij}) - (r_{ij}^2 + x_{ij}^2) \frac{P_{ij}^2 + Q_{ij}^2}{V_i^2}. \quad (4)$$

The nonlinear part in the equations above, i.e.,  $\frac{P_{ij}^2 + Q_{ij}^2}{V_i^2}$ , corresponds to the power losses  
 in the system, which are assumed to be zero in our work. Thus, we have:

$$M_0^\top [V_1 V^\top]^\top = m_0 + M^\top V = D_r P + D_x Q, \quad (5)$$

250 where  $M^0 \in \mathbb{R}^{N \times (N-1)}$ . More specifically, its  $l^{\text{th}}$  column corresponds to one line segment  
 251  $(i, j) \in \mathcal{L}'$ , the entries of which are all zero except for the  $i^{\text{th}}$  and  $j^{\text{th}}$  ones, where  $M_{il}^0 = 1$   
 252 and  $M_{jl}^0 = -1$  when  $j \in N_i$ , i.e., bus  $i$  is closer to the feeder head.  $m_0^\top$  corresponds to  
 253 the first row of  $M^0$  and denotes the slack bus while the rest of the matrix is shown by  
 254  $M$  with the size of  $(N - 1) \times (N - 1)$  [35]. We assume  $V_1 = 1$  and define the vectors  
 255  $[V_i : \forall i \in \{\mathcal{N} / 1\}]$ ,  $P = [P_{ij} : \forall (i, j) \in \mathcal{L}']$ ,  $Q = [Q_{ij} : \forall (i, j) \in \mathcal{L}']$ . We define  $D_r$   
 256 and  $D_x$  as  $(N - 1) \times (N - 1)$  diagonal matrices with the  $l^{\text{th}}$  column and row entry that  
 257 corresponds to one line segment  $(i, j) \in \mathcal{L}'$  equal to  $r_{ij}$  and  $x_{ij}$  respectively. Thus, (2)-(4)  
 258 can be written in the form of matrices as:

$$-MP = -p, \quad (6)$$

$$-MQ = -q, \quad (7)$$

$$V = Rp + Xq - M^{-1\top} m_0, \quad (8)$$

259 with  $p = [p_i : \forall i \in \{\mathcal{N} / 1\}]$ ,  $q = [q_i : \forall i \in \{\mathcal{N} / 1\}]$ ,  $R = M^{-1\top} D_r M^{-1}$  and  
 260  $X = M^{-1\top} D_x M^{-1}$ . As can be seen in (8), the relationship between the voltage and real  
 261 power is now linear.

Let us assume a set of  $D$  distribution systems denoted by  $\mathcal{D} = \{1, \dots, D\}$  connected  
 to the transmission system. For each  $d \in \mathcal{D}$  we know the PCC, which is denoted by  
 $k_d$ . The OPF at each distribution system  $d \in \mathcal{D}$  has a goal to minimise the cost of  
 electricity purchased from the transmission system, the cost of distributed resources and  
 the voltage deviation from the reference value. The cost of electricity at the substation  
 for the time period  $\mathcal{T}$  is a function of the LMP at the PCC at time  $t$  denoted by  $\lambda_{k_d}(t)$ ,

and the amount of power purchased from the transmission system at time  $t$ , i.e.,  $P_{\text{grid}}^d(t)$ , and is defined as follows:

$$\sum_{t \in \mathcal{T}} \left( \lambda_{k_d}(t) P_{\text{grid}}^d(t) \Delta t \right). \quad (9)$$

We denote by  $\mathcal{N}_{PV}^d$  the set of PVs connected to distribution system  $d$ . The cost of PV generation resource is formulated as:

$$\sum_{t \in \mathcal{T}} \sum_{i \in \mathcal{N}_{PV}^d} B_{PV_i} P_{PV_i}(t) \Delta t, \quad (10)$$

where  $B_{PV_i}$  is the cost of PV generation at node  $i$ . We denote by  $\mathcal{N}_B^d$  the set of battery systems connected to the distribution system  $d$ . The cost of battery systems is equal to:

$$\sum_{t \in \mathcal{T}} \sum_{i \in \mathcal{N}_B^d} B_{B_i} (P_{B_i}^{\text{ch}}(t) + P_{B_i}^{\text{dis}}(t)) \Delta t, \quad (11)$$

where  $B_{B_i}$  is the cost of the battery system at node  $i$ . We denote by  $P_{B_i}^{\text{ch}}(t)$  the charging power of the battery system at node  $i$  at time  $t$  and by  $P_{B_i}^{\text{dis}}$  the discharging power of the battery system at node  $i$  at time  $t$ . The voltage deviation from some reference value is defined as follows:

$$\sum_{i \in \mathcal{N}} \sum_{t \in \mathcal{T}} \alpha (V_i(t) - V_{\text{ref}})^2, \quad (12)$$

262 where  $\alpha$  is the voltage regulation cost and  $V_{\text{ref}}$  is the voltage reference value. The  
 263 constraints of the distribution system OPF include the maximum and minimum limits  
 264 for the decision variables:

$$P_{PV,i}^{\text{min}} \leq P_{PV_i}(t) \leq P_{PV,i}^{\text{max}}, i \in \mathcal{N}_{PV}, t \in \mathcal{T}, \quad (13)$$

$$P_{B,i}^{\text{ch,min}} \leq P_{B_i}^{\text{ch}}(t) \leq P_{B,i}^{\text{ch,max}}, i \in \mathcal{N}_B, t \in \mathcal{T}, \quad (14)$$

$$P_{B,i}^{\text{dis,min}} \leq P_{B_i}^{\text{dis}}(t) \leq P_{B,i}^{\text{dis,max}}, i \in \mathcal{N}_B, t \in \mathcal{T}, \quad (15)$$

$$V_i^{\text{min}} \leq V_i(t) \leq V_i^{\text{max}}, i \in \mathcal{N}, t \in \mathcal{T}, \quad (16)$$

$$P_{\text{grid}}^{d,\text{min}} \leq P_{\text{grid}}^d(t) \leq \sum_{i \in \mathcal{I}_k} P_{G_i}(t), t \in \mathcal{T}, \quad (17)$$

where  $P_{\text{grid}}^{d,\text{min}}$  is defined by the interchange flow limit between the distribution system  $d$  and the transmission system. We model the battery system  $i$  as follows (see, e.g., [36])

$$E_{\text{min},i} \leq \sum_{t \in \mathcal{T}} \left( \eta_{\text{ch},i} P_{B_i}^{\text{ch}}(t) - \frac{1}{\eta_{\text{dis},i}} P_{B_i}^{\text{dis}}(t) \right) \Delta t + E_{0,i} \leq E_{\text{max},i}, \forall i \in \mathcal{N}_B, \quad (18)$$

265 where,  $E_{0,i}$  is the initial value of the energy stored,  $E_{\text{max},i}$  and  $E_{\text{min},i}$  are the maximum  
 266 and minimum energy that can be stored in the battery. The network constraints from  
 267 (6)-(8) for every time step  $t \in \mathcal{T}$  are defined as follows:

$$V(t) = Rp(t) + Xq(t) - M^{-1T} m_0, \quad (19)$$

$$p_i(t) = P_{PV_i}(t) + P_{B_i}^{\text{dis}}(t) - P_{B_i}^{\text{ch}}(t) - P_{\text{load}_i}(t), \forall i \in \mathcal{N}_{PV} \cap \mathcal{N}_B, \quad (20)$$

$$p_i(t) = P_{PV_i}(t) - P_{\text{load}_i}(t), \forall i \in \mathcal{N}_{PV} \setminus \mathcal{N}_B, \quad (21)$$

$$p_i(t) = P_{B_i}^{\text{dis}}(t) - P_{B_i}^{\text{ch}}(t) - P_{\text{load}_i}(t), \forall i \in \mathcal{N}_B \setminus \mathcal{N}_{PV}, \quad (22)$$

$$p_i(t) = -P_{\text{load}_i}(t), \forall i \in \mathcal{N} \setminus \mathcal{N}_{PV} \cap \mathcal{N}_B, \quad (23)$$

$$q_i(t) = -Q_{\text{load}_i}(t), \forall i \in \mathcal{N}, \quad (24)$$

268 where  $P_{\text{load}_i}(t)$  is the real load at bus  $i$  at time  $t$  and  $Q_{\text{load}_i}(t)$  is the reactive load at bus  $i$   
 269 at time  $t$ .

The OPF at the distribution system  $d \in \mathcal{D}$  is formulated as follows:

$$\begin{aligned} & \min_{P_{PV_i}(t), P_{B_i}^{\text{ch}}(t), P_{B_i}^{\text{dis}}(t), V_i(t), P_{\text{grid}}^d(t)} (9) + (10) + (11) + (12) \\ & \text{subject to (13) – (24)}. \end{aligned} \quad (25)$$

270

### 271 3. Proposed Coordination Schemes

272 In this section, we formulate the proposed decentralised and centralised schemes  
 273 and discuss the benefits of each approach.

#### 274 3.1. Decentralised Scheme

We define for each distribution system  $d$  the set of decision variables  $y_d$  and the vector  $y = \cup_{d \in \mathcal{D}} y_d$  representing all distribution systems connected to the transmission system. The proposed decentralised scheme is based on solving the following optimisation problem:

$$\begin{aligned} & \min_x f_1(x, y) \\ & \text{subject to } g_1(x, y) \leq 0, \\ & \quad h_1(x, y) = 0, \\ & \quad y_d \in \arg \min_{y_d} \{f_2(x, y_d) : g_2(x, y_d) \leq 0, h_2(x, y_d) = 0\}, \forall d \in \mathcal{D}, \end{aligned} \quad (26)$$

275 where  $f_1(x, y)$  in our problem is the objective function of the TSO OPF, i.e.,  $\sum_{i \in \mathcal{S}} c_i(t) +$   
 276  $\pi \sum_{\ell \in \mathcal{L}} (\theta_n(t) - \theta_m(t))^2$  as described in Section 2.1. Similarly,  $g_1(x, y)$  and  $h_1(x, y) = 0$   
 277 are the equality and inequality constraints of (1) evaluated at  $y$ . In the lower-level  
 278 parametric optimisation problem for each distribution system  $d$ ,  $f_2(x, y_d)$ ,  $g_2(x, y_d)$ ,  
 279 and  $h_2(x, y_d)$  are the collection of distribution level objective functions, equality and  
 280 inequality constraints respectively as defined in (25).

281 This problem is a bi-level optimisation [37]. Such problems were introduced when  
 282 Stackelberg (see, e.g., [38]) formulated a strategic game in 1934 where a leader and a  
 283 follower make sequential moves, starting with the leader. Thus, the upper level and  
 284 lower level can be considered as leader and follower. More specifically, bi-level optimi-  
 285 sation problems are defined where one or some of the decision variables are constrained  
 286 to the solutions of another optimisation problem. Then, the problem is formulated as  
 287 in (26) in two levels of optimisation. Solving bi-level optimisation problems has been  
 288 known to be NP-hard [39]. There are basically two main techniques for solving bilevel  
 289 optimisation problems. The first one keeps the bi-level structure and treats the lower  
 290 level (LL) problem as a parametric optimisation problem that is being solved when-  
 291 ever the solution algorithm for the upper level (UL) problem requires it. The second  
 292 technique is based on the formulation of first order necessary optimality conditions  
 293 for the lower level problem. The lower level problem is then replaced by its necessary  
 294 conditions, which are considered as constraints in the upper level problem. This reduces  
 295 the bi-level problem to a single level nonlinear optimisation problem. The drawback  
 296 of this method is that, in general, necessary conditions are not sufficient for optimality  
 297 and hence information is lost in the single level formulation, which, in turn, may result  
 298 in non-optimal solutions for the bi-level optimisation problem. In particular, the the  
 299 Karush-Kuhn-Tucker (KKT) conditions that should be satisfied in this approach are only  
 300 guaranteed if the optimisation problem is convex [40].

301 In this paper, we propose an approach that resembles the first one discussed above,  
 302 but we treat the two levels as coupled optimisation problems, while iteratively solving

303 one after the other. That is the LL optimisation problem is treated as interdependent  
 304 parametric optimisation problems that are solved whenever the solution algorithm for  
 305 the UL requires it. In particular, the TSO and DSO collaborate to operate the power  
 306 network optimally. Initially, the TSO optimises the transmission system, considering a  
 307 feasible solution of the distribution system initial load. The distribution system's entire  
 308 load is met by the transmission system's resources, i.e., the distribution system does  
 309 not use its distributed resources to meet the load. The TSO solves its own augmented  
 310 DC OPF and announces the locational marginal price of the PCC to the DSO. Next, the  
 311 DSO solves its own LL problem taking into account the capabilities of the distributed  
 312 resources. In the next iteration, the DSO net load is different and the amount of energy  
 313 that DSO buys from the TSO may be reduced, depending on cost. We iterate between  
 314 these two levels until a convergence criterion is met, e.g., that the infinity norm of the  
 315 vector containing the LMP differences between the current iteration and the previous  
 316 iteration does not change by some tolerance. The proposed algorithm is described as  
 317 follows:

---

**Algorithm** Iterative algorithm for solving (26)

---

1: **Initialization**

2: Set  $\nu = 0$ .

3: Consider  $y_d[0]$  so that it is a feasible solution of the LL optimisation  $\forall d \in \mathcal{D}$ .

4: **Repeat until convergence**

5: Solve the UL optimisation problem using  $y_d[\nu]$ ; let the solution be  $x[\nu]$  and  $\lambda_{k_d}[\nu]$ .

6: Solve the LL optimisation for  $x[\nu]$  using  $\lambda_{k_d}[\nu]$ . Let the solution be  $y_d[\nu + 1], \forall d \in \mathcal{D}$ .

7: Set  $\nu \leftarrow \nu + 1$  and go to step (4).

---

318 Considering this iterative procedure, the LL and UL optimisation problems are  
 319 solved the same number of times and the levels are treated as uncoupled problems, just  
 320 coupled at the interface by the procedure. There is no formal proof of convergence for  
 321 such an iterative scheme, however convergence has been experimentally shown [41]. We  
 322 further demonstrate that the proposed algorithm converges to a near optimal solution.  
 323 The flowchart of the algorithm is given in Fig. 1.

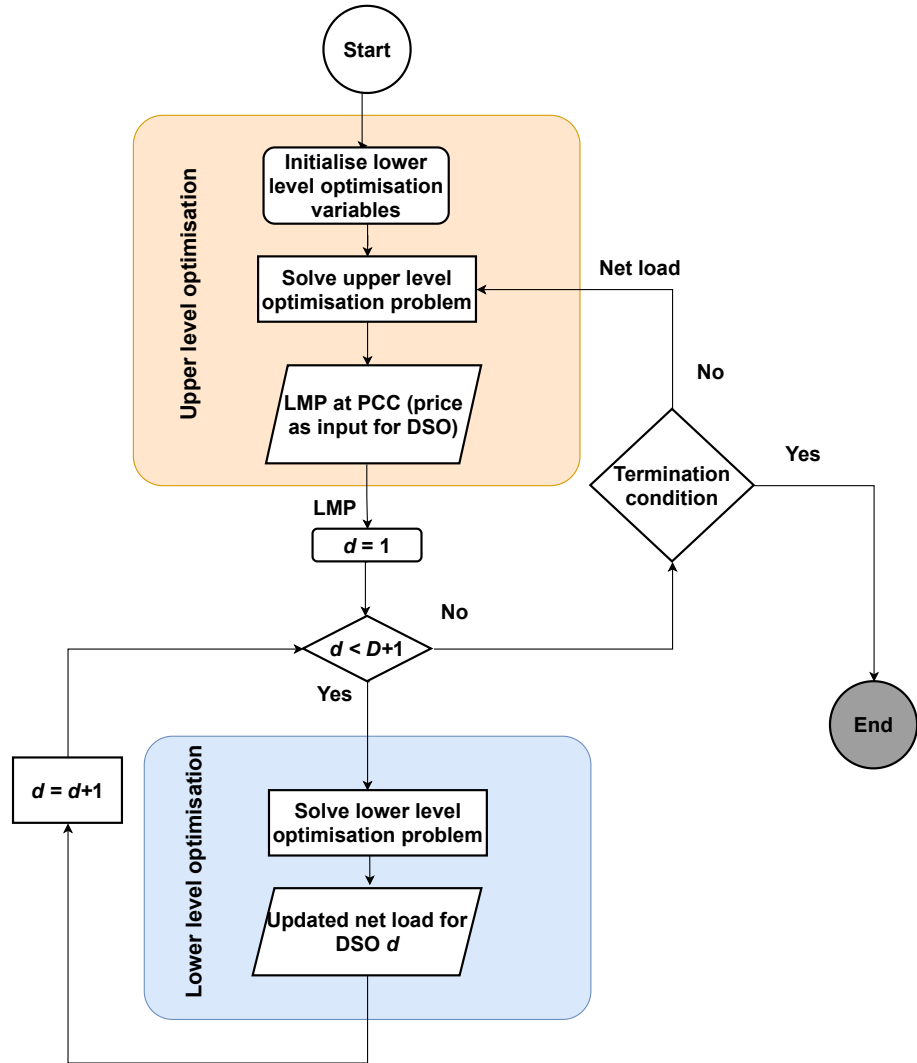


Figure 1. Decentralised iterative scheme flowchart.

### 324 3.2. Centralised Scheme

This coordination scheme introduces the TSO as a leader who operates the transmission and distribution systems as one entire power network. In this case, the TSO solves a multi-objective optimisation (MOO) problem which can be formulated as follows:

$$\begin{aligned}
 & \min_{x,y} (f_1(x,y), f_2(x,y)) \\
 & \text{subject to } g_1(x,y) \leq 0, \\
 & \quad g_2(x,y) \leq 0, \\
 & \quad h_1(x,y) = 0, \\
 & \quad h_2(x,y) = 0,
 \end{aligned} \tag{27}$$

where  $x$  represents the decision variables for the transmission system and  $y$  the decision variables for all distribution systems. The first objective,  $f_1(x,y)$ , incorporates the TSO objective functions, and  $f_2(x,y)$  the objective functions of all the distribution systems in  $\mathcal{D}$ , that is, (10) + (11) + (12) as described in (1) and (25) respectively. The inequality and equality constraints are denoted as  $g_1(x,y), g_2(x,y)$  and  $h_1(x,y), h_2(x,y)$  respectively. The notion of “optimality” in solving MOO problems is known as Pareto optimal. A solution is said to be Pareto optimal if there is no way to improve one objective without worsening the other, i.e., the feasible point  $(x^*, y^*)$  is Pareto optimal if there is no other

feasible point  $(x, y)$  such that for all  $i, j$  with  $i \neq j$ ,  $f_i(x, y) = f_i(x^*, y^*)$  with strict inequality in at least one objective,  $f_j(x, y) < f_j(x^*, y^*)$ . However, given their conflicting nature, it is difficult to minimise the objective functions simultaneously, and hence the Pareto solutions usually appear scattered. In solving the optimisation problem (27) we obtain the Pareto front. In general, identifying the set of all Pareto optimality points is not a tractable problem. A common approach for solving MOO is to find many evenly distributed efficient points, and use points to approximate the Pareto front. In this paper, we use the weighted sum method (see, e.g., [42], [43]) to convert the MOO into a single objective optimisation problem by using a convex combination of objectives. More formally, the weighted sum method solves the following scalar optimisation problem:

$$\begin{aligned}
 & \min_{x, y} w_1 f_1(x, y) + w_2 f_2(x, y) \\
 & \text{subject to } g_1(x, y) \leq 0, \\
 & \quad g_2(x, y) \leq 0, \\
 & \quad h_1(x, y) = 0, \\
 & \quad h_2(x, y) = 0 \\
 & \quad w_1 + w_2 = 1, \\
 & \quad w_1, w_2 \geq 0.
 \end{aligned} \tag{28}$$

325 By appropriately changing the weight vector  $w = [w_1, w_2]^\top$  we can approximate the  
 326 Pareto front. The weight  $w_2$  corresponds to all  $d \in \mathcal{D}$  distribution systems. We assign  
 327 equal weights to each distribution system, i.e.,  $w_2 = \sum_{d \in \mathcal{D}} w_{2d}$ , where  $w_{2d} = \frac{w_2}{|\mathcal{D}|}$ ,  $\forall d \in \mathcal{D}$   
 328 with  $|\mathcal{D}|$  the cardinality of the set  $\mathcal{D}$ . Our problem has a convex Pareto front, hence we  
 329 can generate all points of the Pareto front. Using the proposed method we investigate  
 330 how the objectives of TSO and DSOs interact with each other, and the TSO directly  
 331 manages the entire system and purchases power from distributed energy sources in  
 332 the distribution system; as for bidirectional power flows, if distributed energy sources  
 333 generate excess energy needed at the distribution system level is fed into the transmission  
 334 system.

#### 335 4. Numerical Results

336 We present several numerical examples to demonstrate the capabilities of the pro-  
 337 posed framework. We discuss the properties of the proposed decentralised coordination  
 338 scheme in terms of convergence with some sensitivity studies. Insights are provided  
 339 into both proposed coordination schemes. Furthermore, we demonstrate the interaction  
 340 of TSOs and DSOs with the determination of the Pareto front of the centralised optimisa-  
 341 tion problem. Thus, in Section 4.1, the case study information is provided, followed by  
 342 the numerical results of decentralised and centralised schemes in Sections 4.2 and 4.3,  
 343 respectively.

##### 344 4.1. System Description

345 To validate the proposed framework we need to construct a power system with  
 346 many voltage levels that will represent the transmission and distribution systems. As  
 347 such, we select a five-node transmission system on which four distribution system  
 348 feeders are connected to different nodes as depicted in Fig. 2.

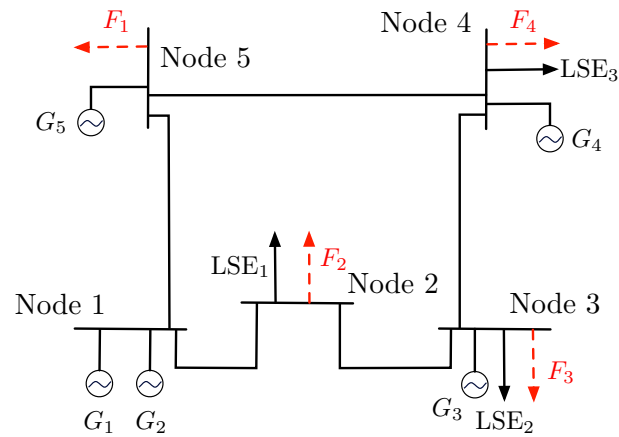


**Figure 2.** Transmission and distribution system.

349 We denote by  $F_i$  the  $i_{th}$  feeder connected to the transmission system. More speci-  
 350 cally,  $F_1$  and  $F_3$  correspond to the IEEE standard 33 bus feeder and  $F_2$  and  $F_4$  to the 69  
 351 IEEE standard bus feeder [44–46]. The load serving entities at a transmission node  $i$  are  
 352 denoted by  $LSE_i$ . There are five generators connected at the transmission level in nodes  
 353 1, 3, 4 and 5. The transmission system data may be found in [24]. To demonstrate how  
 354 the TSO-DSO coordination schemes can facilitate the integration of DG we modify the  
 355 standard IEEE 33 and 69 bus feeders by deploying PV and battery systems at different  
 356 nodes. We assume that the distributed resources are mostly installed at end-nodes in the  
 357 distribution level where the voltage drop levels are worst [47]. The modified feeders are  
 358 depicted in Figs. 3, 4, respectively. In particular, PV and battery systems are installed in  
 359 nodes 18, 22, 25 and 33 in the 33 bus feeder and in nodes 2, 3, 27, and 64 in the IEEE 69  
 360 bus feeder. The distributed resources data are presented in Table 1. Also, we assume that  
 361 each node's voltage in the distribution system is bounded between 0.95 pu and 1.05 pu.

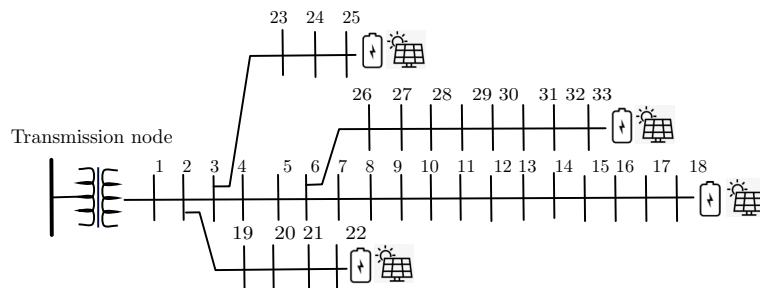


**Figure 3.** Modified IEEE 33 bus distribution feeder.

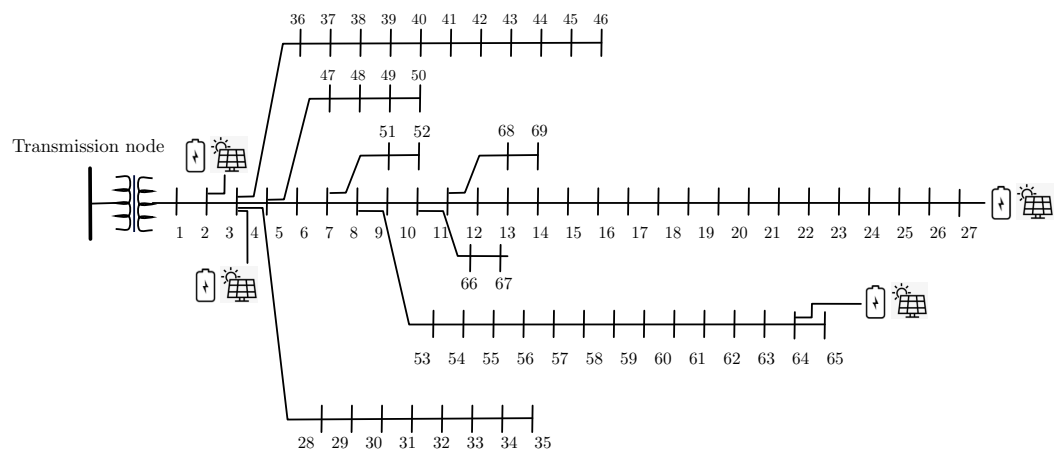


**Figure 4.** Modified IEEE 69 bus distribution feeder.

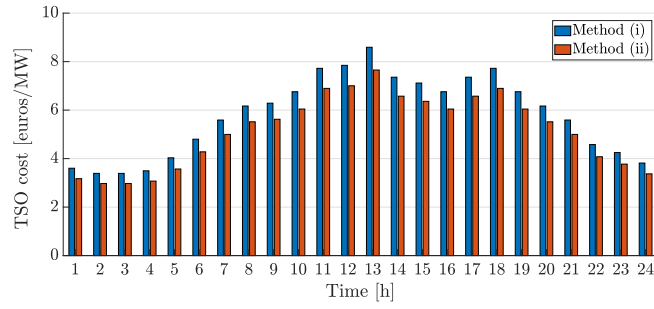
Feeder	Variable	Value	Unit
All	$P_{PV}^{\min}$	0	MW
All	$P_{PV}^{\max}$	30	MW
All	$B_{PV}$	2.584	€/MW
$F_1, F_3$	$P_B^{\text{dis},\min}$	0	MW
$F_1, F_3$	$P_B^{\text{dis},\max}$	30	MW
$F_1, F_3$	$P_B^{\text{ch},\min}$	0	MW
$F_1, F_3$	$P_B^{\text{ch},\max}$	30	MW
$F_1, F_3$	$B_B^{\text{dis},\min}$	0.380	€/MW
$F_2, F_4$	$P_B^{\text{dis},\min}$	0	MW
$F_2, F_4$	$P_B^{\text{dis},\max}$	15	MW
$F_2, F_4$	$P_B^{\text{ch},\min}$	0	MW
$F_2, F_4$	$P_B^{\text{ch},\max}$	15	MW
$F_2, F_4$	$B_B^{\text{dis},\min}$	0.380	€/MW
$F_1, F_3$	$P_{\text{grid}}^{\min}$	-110	MW
$F_2, F_4$	$P_{\text{grid}}^{\min}$	-60	MW

Table 1: Distributed resources' physical limits and bid information.

362 Next, we implement both the proposed centralised and the decentralised schemes,  
 363 we compare the results with current practise, which refers to when the TSO solves its  
 364 OPF and determines the LMPs at the substations. Next, the DSOs dispatch distributed  
 365 DG by optimising cost and considering the LMP at the substation as a fixed parameter.  
 366 In current practise there is minimal coordination between TSOs and DSOs. The three  
 367 methodologies are compared against a variety of metrics; these are: total cost; hourly  
 368 LMPs; hourly DG output; hourly generator output at the transmission level; net load;  
 369 and level of congestion.

#### 370 4.2. Decentralised Coordination Scheme

371 We apply the scheme proposed in Section 3.1 to the system described above. In order  
 372 to demonstrate how the decentralised scheme facilitates the integration of distributed  
 373 energy resources we compare its optimal operation (method (ii)) against current practice  
 374 (method (i)), where the current practise as discussed in the introduction section is when  
 375 the TSO solves its own OPF and determines the LMPs at the substation, and the DSOs  
 376 dispatch DG by optimising cost and considering the LMP at the substation as a fixed  
 377 parameter. We run both cases for a one day period with hourly intervals. In Fig. 5, the  
 378 TSO operation cost for both cases is depicted. We notice that the proposed decentralised  
 379 coordination scheme results in a reduced transmission operation cost for all hours of  
 380 the day. The reason is that distributed energy resources, which are less expensive than  
 381 generators connected at the transmission level, are used to a greater extent as seen in  
 382 Fig. 6.



**Figure 5.** Transmission operation cost for methods (i) current practise and (ii) proposed decentralised TSO-DSO coordination scheme.

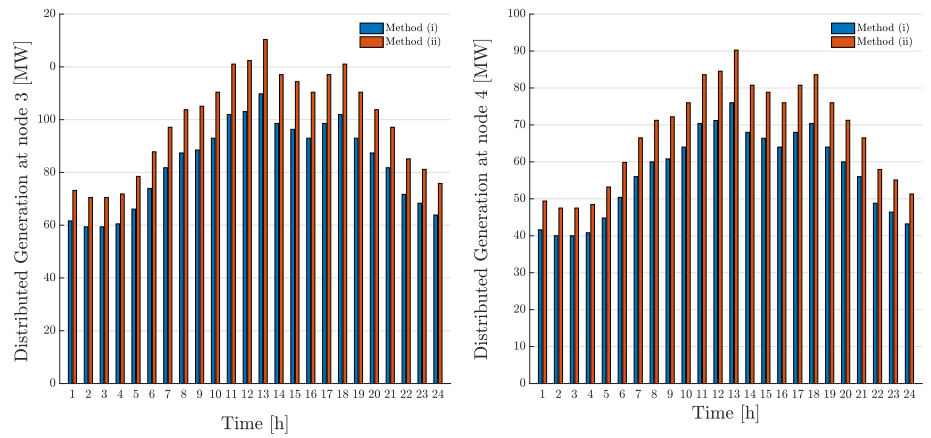


**Figure 6.** The total amount of distributed generation for methods (i) current practise and (ii) proposed decentralised TSO-DSO coordination scheme at nodes 3 and 4.

Another effect of the increasing use of distributed resources is that they relieve the congestion that is present in the transmission system, which in turn reduces TSO operational costs. For method (i) the LMPs for each hour at each node may be found in Table 2. We notice that for the same hour each node has a different LMP. This demonstrates, based on the formulation of the augmented DCOPF in (1), that some line flows have reached their limits. The LMPs of method (ii) are shown in Table 3. We notice that the LMP difference between hours has been reduced, reflecting the fact that there is less congestion in the transmission system. In fact the LMPs are practically the same for all nodes at every hour when the proposed decentralised scheme is implemented. Following the formulation of (1) and using the KKT conditions of optimality, the LMP difference is expressed as a function of the congestion that can be present in the network, i.e., (see, e.g., [48]):

$$\lambda_k - \lambda_{k'} = \sum_{\ell \in \mathcal{L}} \phi_{\ell}^{\{k,k'\}} \mu_{\ell}, \quad (29)$$

383 where  $\mu_{\ell}$  is the dual variable of the power flow limits for line  $\ell$ ;  $\mathcal{L}$  is the subset of lines  
 384 that are at their limits, i.e.,  $\mathcal{L} = \{\ell_i : i = 1, \dots, L, \mu_{\ell_i} \neq 0\}$ ; and  $\phi_{\ell}^{\{k,k'\}}$  is the power  
 385 transfer distribution factor of transaction with node pair  $\{k, k'\}$  with respect to line  $\ell$ .  
 386 We can interpret (29) physically by considering an injection at node  $k$  and its withdrawal  
 387 at node  $k'$ . We interpret  $\phi_{\ell}^{\{k,k'\}}$  as the fraction of the transaction with node pair  $\{k, k'\}$   
 388 of 1 MW that flows on line  $\ell$ . As such for every hour the LMP differences are purely a  
 389 function of the transmission usage costs of the congested lines, thus showing the “level”  
 390 of congestion.

Hour	Node 1	Node 2	Node 3	Node 4	Node 5
1	12.67	28.15	25.22	17.15	13.46
2	12.62	28.01	25.10	17.08	13.41
3	12.62	28.01	25.10	17.08	13.41
4	12.64	28.08	25.16	17.11	13.44
5	12.76	28.42	25.45	17.30	13.56
6	12.93	28.89	25.87	17.55	13.74
7	13.09	29.36	26.28	17.80	13.92
8	13.21	29.70	26.58	17.99	14.05
9	13.23	29.77	26.64	18.02	14.08
10	13.32	30.04	26.88	18.17	14.18
11	13.51	30.58	27.35	18.46	14.39
12	13.53	30.65	27.41	18.49	14.41
13	13.68	31.05	27.76	18.71	14.57
14	13.44	30.38	27.17	18.35	14.31
15	13.39	30.24	27.05	18.28	14.26
16	13.32	30.04	26.88	18.17	14.18
17	13.44	30.38	27.17	18.35	14.31
18	13.51	30.58	27.35	18.46	14.39
19	13.32	30.04	26.88	18.17	14.18
20	13.21	29.70	26.58	17.99	14.05
21	13.09	29.36	26.28	17.80	13.92
22	12.88	28.75	25.75	17.48	13.69
23	12.81	28.55	25.57	17.37	13.62
24	12.71	28.28	25.34	17.22	13.51

Table 2: Locational marginal prices for method (i): current practise for TSO-DSO coordination in €/MW.

Hour	Node 1	Node 2	Node 3	Node 4	Node 5
1	12.27	12.28	12.28	12.27	12.27
2	12.13	12.14	12.14	12.14	12.13
3	12.13	12.14	12.14	12.14	12.13
4	12.20	12.21	12.21	12.21	12.20
5	12.54	12.55	12.55	12.54	12.54
6	13.01	13.02	13.02	13.01	13.01
7	12.55	28.14	25.19	17.06	13.35
8	12.88	12.89	12.89	12.88	12.88
9	12.90	12.91	12.91	12.90	12.90
10	12.98	12.99	12.99	12.99	12.98
11	13.15	13.16	13.16	13.15	13.15
12	13.17	13.18	13.18	13.17	13.17
13	11.93	11.94	11.94	11.94	11.93
14	13.08	13.10	13.10	13.09	13.08
15	13.04	13.06	13.06	13.05	13.04
16	12.98	12.99	12.99	12.99	12.98
17	13.08	13.10	13.10	13.09	13.08
18	13.15	13.16	13.16	13.15	13.15
19	12.98	12.99	12.99	12.99	12.98
20	12.88	12.89	12.89	12.88	12.88
21	12.55	28.14	25.19	17.06	13.35
22	12.87	12.89	12.89	12.88	12.87
23	12.67	12.68	12.68	12.68	12.67
24	12.40	12.41	12.41	12.41	12.40

Table 3: Locational marginal prices for method (ii): proposed decentralised TSO-DSO coordination in €/MW.

391 In Tables 4, 5 the hourly power output of each transmission generator is shown. We  
392 notice that with method (ii) the total power used by generators at the transmission level  
393 is reduced compared to method (i). The reason is that the less expensive distributed  
394 generators at distribution level are used to satisfy the load instead. More specifically,  
395 we notice that with method (ii) the transmission level generators 2, 3, and 4 have zero  
396 output for most hours of the day since they are the most expensive ones.

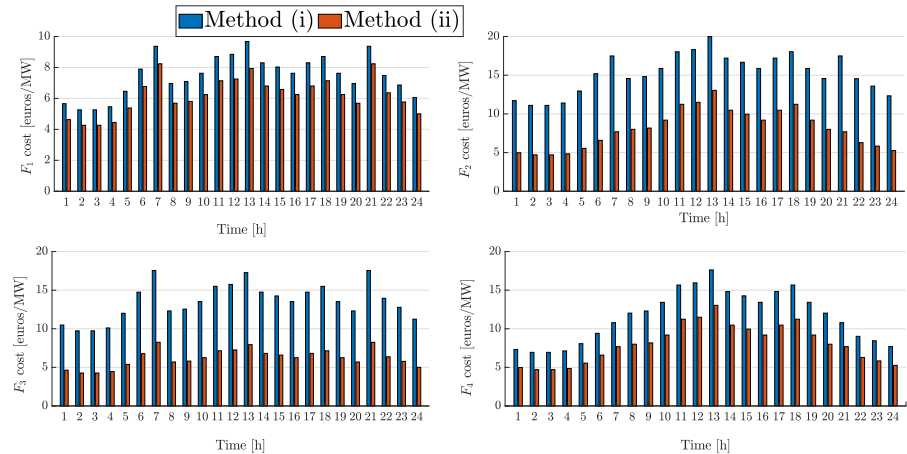
Hour	$P_{G_1}$	$P_{G_2}$	$P_{G_3}$	$P_{G_4}$	$P_{G_5}$
1	110	18.53	19.52	0	110
2	110	15.09	13.36	0	110
3	110	15.09	13.36	0	110
4	110	16.81	16.44	0	110
5	110	25.41	31.84	0	110
6	110	37.45	53.39	0	110
7	110	49.5	74.95	0	110
8	110	58.1	90.35	0	88.4
9	110	59.82	93.43	0	90.88
10	110	60	110	2.45	100.81
11	110	43.78	110	57.07	110
12	94.58	60.36	110.71	60	110
13	62.8	0.03	116.72	42.99	110
14	110	55.25	110	31.2	110
15	110	60	110	16.85	108.26
16	110	60	110	2.45	100.81
17	110	55.25	110	31.2	110
18	110	43.78	110	57.07	110
19	110	60	110	2.45	100.81
20	110	58.1	90.35	0	88.4
21	110	49.5	74.95	0	110
22	110	34.01	47.23	0	110
23	110	28.85	38	0	110
24	110	21.97	25.68	0	110

Table 4: The power output in MW of generators at the transmission level for method (i): current practise for TSO-DSO coordination.

Hour	$P_{G_1}$	$P_{G_2}$	$P_{G_3}$	$P_{G_4}$	$P_{G_5}$
1	39.14	0	0	0	110
2	30.02	0	0	0	110
3	30.02	0	0	0	110
4	34.58	0	0	0	110
5	57.38	0	0	0	110
6	89.3	0	0	0	110
7	107.99	6.66	6.58	0	110
8	82.98	0	0	0	88.4
9	85.82	0	0	0	90.88
10	91.19	0	0	0	100.81
11	101.05	0.88	0	0	110
12	101.78	1.49	0	0	110
13	9.58	0	0	0	110
14	97.9	0	0	0	110
15	95.22	0	0	0	108.26
16	91.19	0	0	0	100.81
17	97.9	0	0	0	110
18	101.05	0.88	0	0	110
19	91.19	0	0	0	100.81
20	82.98	0	0	0	88.4
21	107.99	6.66	6.58	0	110
22	80.18	0	0	0	110
23	66.5	0	0	0	110
24	48.26	0	0	0	110

Table 5: The power output in MW of generators at the transmission level for method (ii): proposed decentralised TSO-DSO coordination.

397 In Fig. 7 we depict the operational cost for each distribution feeder connected to  
398 different nodes of the transmission system for methods (i) and (ii). We notice that the  
399 proposed coordination scheme results in reduced costs for all DSOs since all resources  
400 were utilised in a more efficient way as discussed above.



**Figure 7.** The cost for each feeder for methods (i) and (ii).

401 We now study the net load at the transmission nodes using both methods. We can  
 402 see in Fig. 8 that the net loads at the transmission system at nodes 2 and 3 decrease, a  
 403 fact that is also reflected in the OPF in the transmission system and its LMPs. We also  
 404 notice that there is a sharp fall and rise in the net load, between hours 7 and 8 and 20  
 405 and 21 respectively. This is due to the fact that the power flow between nodes 1 and 2 at  
 406 time 7 and 21 is 75 MW, which is equal to the line's thermal limit. This causes the LMP  
 407 divergence in these hours, as shown in Table 3.

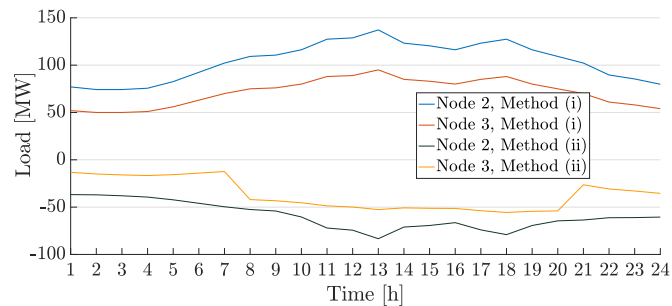


**Figure 8.** Net load at nodes 2,3 with using methods (i) and (ii).

408 Last, we depict the hourly operational cost for the TSO and the DSOs in Fig. 9 which  
 409 will be used to compare the two proposed schemes.

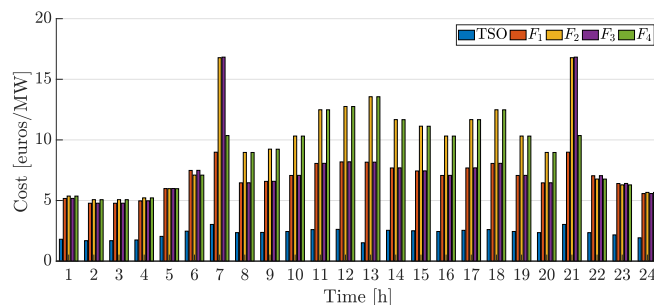


**Figure 9.** TSO and DSOs operational cost using the proposed decentralised coordination scheme.

410 We next check the convergence properties of the proposed algorithm. In Figs. 10, 11  
 411 we illustrate the evolution of the hourly objective functions of  $F_2$  and the transmission  
 412 system for a 24-hour period with respect to the iteration numbers of algorithm. We notice  
 413 that the algorithm converges after three iterations. To test the sensitivity of the proposed  
 414 algorithm with respect to the initial point, i.e., the choice of initial load value for the

415 distribution system, we changed the initial point to be full load, 85%, 75%, and 65% of  
 416 the full load. In all cases the algorithm converges in three iterations. Next, to analyse the  
 417 sensitivity of the proposed algorithm with respect to the level of distributed resources  
 418 penetration we depict in Fig. 12 the evolution of  $F_2$  hourly cost for two different levels  
 419 of penetration with the same initial point (step 3 of the algorithm) with respect to the  
 420 number of iterations. The final cost is different for the two cases since there are hours  
 421 where the DG price is smaller than the grid price and vice versa.

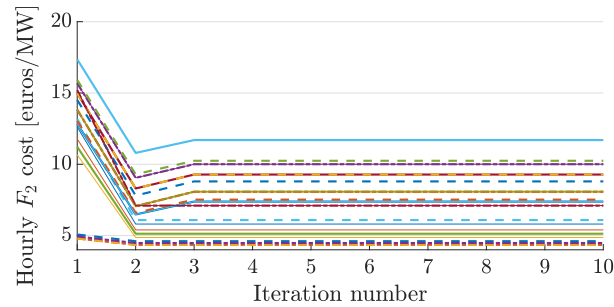


**Figure 10.** Evolution of the hourly cost for  $F_2$  with respect to the iteration number.

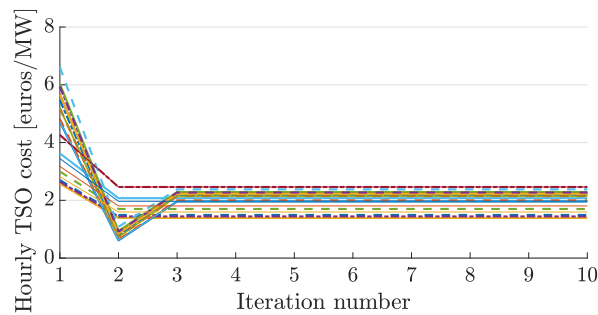


**Figure 11.** Evolution of the hourly cost for the transmission system with respect to the iteration number.

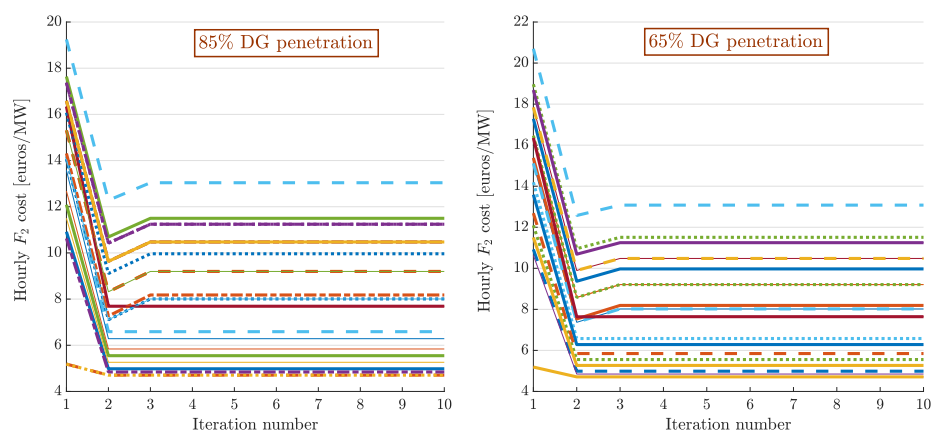


**Figure 12.** Evolution of hourly cost for  $F_2$  for different penetration levels of distributed generation.

#### 422 4.3. Centralised Coordination Scheme

423 We apply the proposed scheme developed in Section 3.2 to the system described in  
 424 Fig. 2. In order to demonstrate how the proposed centralised scheme can facilitate the  
 425 integration of distributed energy resources we compare method (i), which is the optimal  
 426 operation with the current practise, with method (iii), which is the proposed centralised

427 scheme. We start the simulation by assigning the same weights to the transmission  
 428 cost function and the distribution feeders' cost functions as  $w_1 = w_2 = 0.5$ . The TSO  
 429 cost as depicted in Fig. 13 is reduced significantly with method (iii), i.e., the centralised  
 430 scheme, in comparison to the current practise due to the increase in the integration of  
 431 the distributed resources at different nodes as shown in Fig. 14.

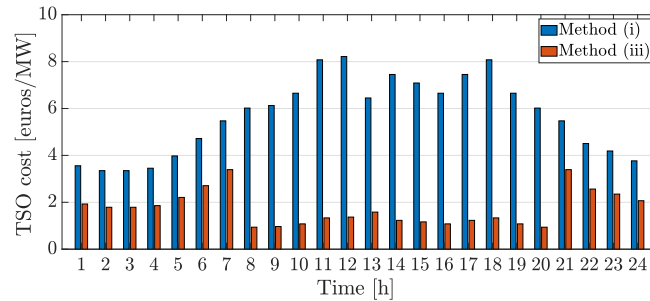


**Figure 13.** Transmission operation cost for methods (i) current practise and (iii) proposed centralised TSO-DSO coordination scheme.

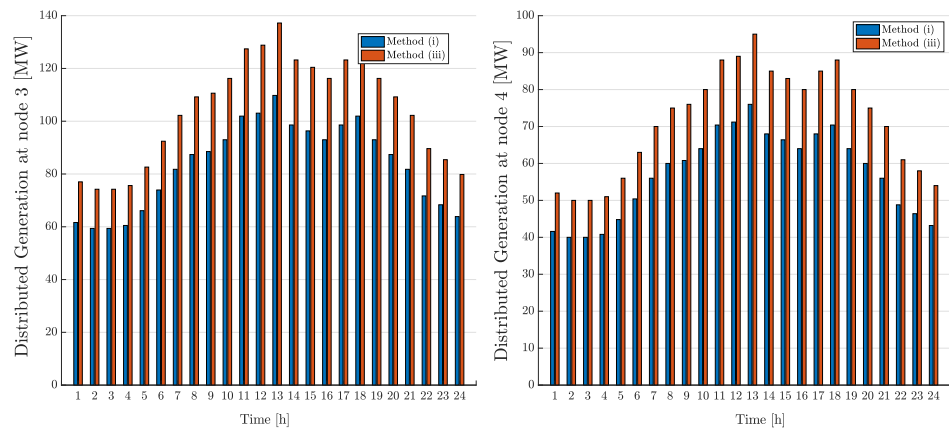


**Figure 14.** The total amount of distributed generation for methods (i) current practise and (iii) proposed centralised TSO-DSO coordination scheme at nodes 3 and 4.

432 In Fig. 15 the net load at the transmission level using methods (i) and (iii) is depicted.  
 433 We notice that it is more cost efficient for the TSO to purchase power from the DG that is  
 434 present in the distribution systems. For instance, the negative load at node 2 means that  
 435 the excess power of the distributed resources is redirected to the transmission system.  
 436 DGs usually sell at a price equal to the LMP at their PCC. That results in distributed  
 437 resources' owners gaining revenue by selling power to the TSO, while the TSO also  
 438 meets its load at a lower cost. In Fig. 16 the operational cost for each hour for the TSO  
 439 and DSOs for the proposed centralised coordination scheme is depicted. Fig. 16 shows  
 440 that the transmission cost for method (iii) with  $w_1 = w_2 = 0.5$  is lower than that of  
 441 method (ii) as depicted in Fig 9. The difference is that more power is being used from  
 442 the DGs in method (iii) compared to that of method (ii). However, we notice that the  
 443 cost of feeders in method (iii) is higher than that of method (ii). Again, this is due to the  
 444 fact that more power is being used from the DGs in method (iii) compared to that of  
 445 method (ii). These values can be used by DSOs and TSOs to formulate their bids and  
 446 provide incentives for DG participation respectively.

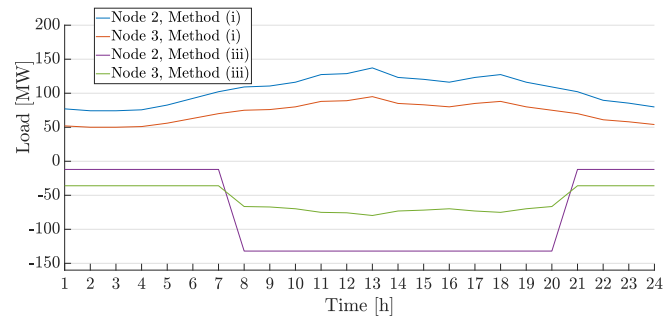


Figure 15. Net load at nodes 2,3 with using methods (i) and (iii).

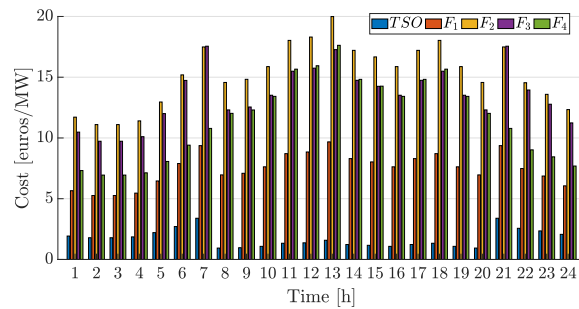


Figure 16. TSO and DSOs operational cost using the proposed centralised coordination scheme.

Hour	$P_{G_1}$	$P_{G_2}$	$P_{G_3}$	$P_{G_4}$	$P_{G_5}$
1	52.05	0	0	0	110
2	42.45	0	0	0	110
3	42.45	0	0	0	110
4	47.25	0	0	0	110
5	71.25	0	0	0	110
6	102.64	2.2	0	0	110
7	110	10.87	17.58	0	110
8	0	0	0	0	88.4
9	0	0	0	0	90.88
10	0	0	0	0	100.81
11	10.67	0	0	0	110
12	13.15	0	0	0	110
13	28.05	0	0	0	110
14	3.22	0	0	0	110
15	0	0	0	0	108.26
16	0	0	0	0	100.81
17	3.22	0	0	0	110
18	10.67	0	0	0	110
19	0	0	0	0	100.81
20	0	0	0	0	88.4
21	110	10.87	17.58	0	110
22	95.25	0	0	0	110
23	80.85	0	0	0	110
24	61.65	0	0	0	110

Table 6: The power output in MW of generators at the transmission level for method (iii): proposed centralised TSO-DSO coordination.

447 The hourly power output of transmission generators for method (iii) is presented in  
 448 Table 6. We notice that between hours 8 and 20 the distributed resources located in the

449 distribution systems satisfy the load at the transmission level, whereas at night hours  
 450 mostly the TSO is responsible for supplying the load to the customers. This reverse  
 451 power flow also impacts the LMP as shown in Table 7, where we notice a marginal  
 452 increase in the LMPs for the night hours is achieved. Similarly to method (ii) there is  
 453 congestion at hours 7 and 21 due to the congested line between nodes 1 and 2.

Hour	Node 1	Node 2	Node 3	Node 4	Node 5
1	14.52	14.53	14.53	14.53	14.52
2	14.42	14.43	14.43	14.43	14.42
3	14.42	14.43	14.43	14.43	14.42
4	14.47	14.48	14.48	14.48	14.47
5	14.71	14.72	14.72	14.72	14.71
6	15.03	15.04	15.04	15.03	15.03
7	15.13	27.74	25.35	18.78	15.78
8	11.24	11.24	11.24	11.24	11.24
9	11.27	11.27	11.27	11.27	11.27
10	11.41	11.41	11.41	11.41	11.41
11	14.11	14.11	14.11	14.11	14.11
12	14.13	14.13	14.14	14.13	14.13
13	14.28	14.28	14.29	14.28	14.28
14	14.03	14.03	14.04	14.04	14.03
15	11.52	11.52	11.52	11.52	11.52
16	11.41	11.41	11.41	11.41	11.41
17	14.03	14.03	14.04	14.04	14.03
18	14.11	14.11	14.11	14.11	14.11
19	11.41	11.41	11.41	11.41	11.41
20	11.24	11.24	11.24	11.24	11.24
21	15.13	27.74	25.35	18.78	15.78
22	14.95	14.97	14.97	14.96	14.95
23	14.81	14.82	14.82	14.81	14.81
24	14.62	14.63	14.63	14.62	14.62

Table 7: Locational marginal prices for method (iii): proposed centralised TSO-DSO coordination in €/MW.

454 Next, we analyse the interaction between the TSO and the DSOs. For this, we modify  
 455 the weights of (28) to obtain an approximation of the Pareto front. More specifically, we  
 456 start with  $w_1 = 0$  and  $w_2 = 1$ , and with increments of 0.05 we reach  $w_1 = 1$  and  $w_2 = 0$ .  
 457 The Pareto front is depicted in Fig. 17. By moving along the curve, we can minimise  
 458 DSOs' objective at the expense of TSO's objective, or minimise the TSO's objective at the  
 459 expense of DSOs' objective. However we cannot improve both at once, i.e., there is no  
 460 mathematical "best" point along the Pareto front.

461 To provide insights into the potential conflicts between TSOs and DSOs we discuss  
 462 in greater detail the two extreme cases, i.e.,  $w_1 = 0$  and  $w_2 = 1$  and  $w_1 = 1$  and  $w_2 = 0$ .  
 463 The TSO and DSO costs for the first one are 0 €/MW and 500 €/MW, respectively; and  
 464 for the latter they are 140 €/MW and 0 €/MW, respectively. In other words, when the  
 465 objective is to only minimise the TSO cost; all costs are being incurred by the DSOs and  
 466 vice versa. In both cases, all constraints, e.g., voltage and thermal limits, are met thus  
 467 the power system quality is guaranteed.

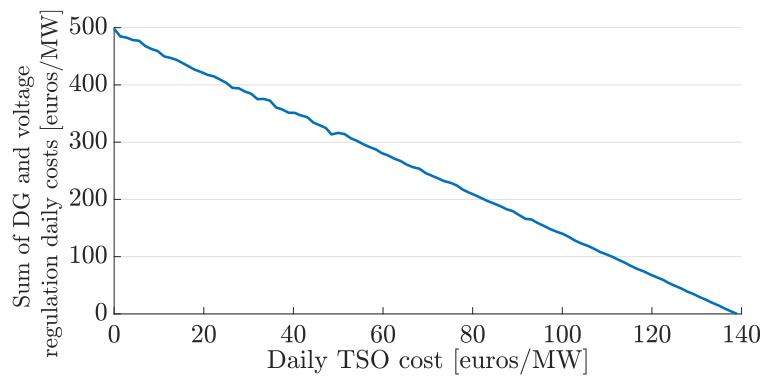


**Figure 17.** Pareto Front of the sum of all feeders DG and voltage regulation daily cost with respect to the TSO cost.

468 In Fig. 18, we depict the total DSO cost that includes the payments to the TSO given  
 469 in (9), DG cost given in (10) and (11), and voltage regulation costs given in (12). We  
 470 compare the results for different weights with methods (i) and (ii). We notice that the  
 471 results of method (ii) are close to the Pareto front offering a near optimal solution. The  
 472 appropriate choice of operation for the Pareto front is a balance of priorities between  
 473 TSOs and DSOs and the determination of specific incentives, which are part of future  
 474 work. Another implication of the Pareto front is that any point in the feasible region  
 475 that is not on the Pareto front is not considered to be a “good” solution, e.g., method (i).  
 476 Either objective, or both, can be improved at no penalty to the other. This demonstrates  
 477 that there a lot of improvements to be made to current TSO-DSO coordination practise,  
 478 i.e., method (i). To determine the priorities of the proposed decentralised scheme we  
 479 have to analyse where its solution lies in the Pareto front. More specifically, we notice in  
 480 Figs. 18 and 19 that the proposed decentralised scheme provides a balance between the  
 481 TSO and DSO objective, since it lies between the two extreme cases.

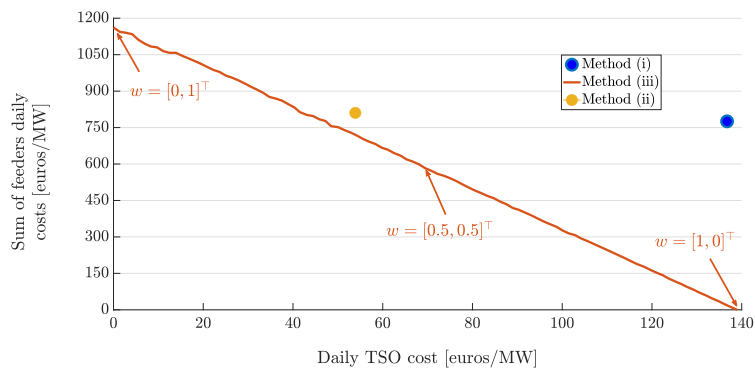


**Figure 18.** Pareto Front of the sum of all feeders daily cost with respect to the TSO cost.

482 Next, we depict in Fig. 19 the daily cost of individual feeders, which includes the  
 483 payments to the TSO, the cost of DG and voltage regulation, to investigate how far  
 484 from the optimal solution each feeder operates for the various schemes. We notice that  
 485 for method (ii)  $F_2$  operates at the optimum,  $F_3$  at a point that is at the expense of other  
 486 feeders and  $F_1$  and  $F_4$  at points further away from the optimal solutions. However, the  
 487 summation of these costs corresponds to a near optimal solution as seen in Fig. 18.

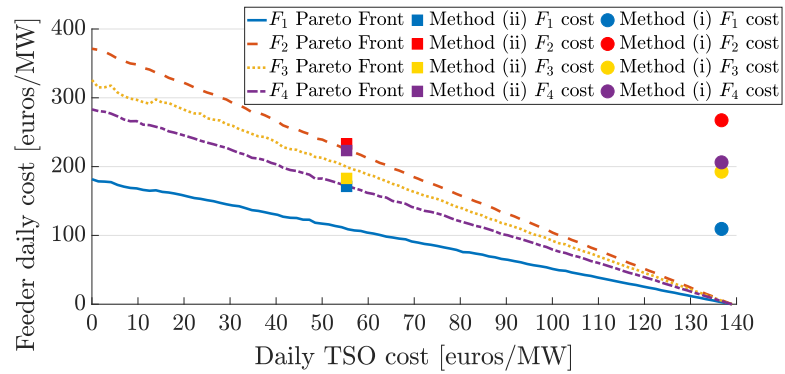


**Figure 19.** Pareto Front of daily cost for  $F_i$ ,  $i = 1, \dots, 4$  with respect to the TSO cost.

488 In both schemes the transmission cost decreases while for method (iii) the trans-  
 489 mission operation cost reduction is higher than that of method (ii). In comparison to  
 490 the current practise, i.e., method (i), both schemes are more effective in terms of the  
 491 share contribution of the distributed generators at each transmission node, while the  
 492 utilisation rate of generation for method (iii) is higher than that of method (ii). Using  
 493 method (iii), we can see that the output of each generator at the transmission level  
 494 is lower than that of method (ii) and for method (ii) is lower than that of method (i).  
 495 Although for method (ii) and method (iii), the congestion level is improved, the LMP  
 496 for each node at each hour is higher at night hours in method (iii). This is due to the  
 497 increased output of transmission generators at night hours. *It should be noted that in all  
 498 case studies all variables, e.g., voltage levels, transmission line flows, are kept within the  
 499 limits of acceptable for power quality purposes as defined by the constraints of the OPFs.*  
 500 For example, voltage levels of each bus in the distribution system at every time interval  
 501 are in the range of 0.95 – 1.05 pu. The algorithm running time for the centralised scheme  
 502 is 12,387 msec and for the decentralised is 21,800 msec in a Windows machine which is  
 503 equipped with AMD<sup>®</sup> FX-9830P RADEON R7 CPU with four Cores at 3.00 GHz and  
 504 16 GB of RAM. As expected the centralised scheme is approximately two times faster;  
 505 however both schemes are fast enough for real-time operation purposes.

## 506 5. Conclusion and discussion

507 In this paper, we have presented a novel TSO-DSO coordination framework that  
 508 increases the efficient use of distributed generation resources. More specifically, we  
 509 have two coordination schemes: one centralised, another decentralised. The underlying  
 510 network for both systems is approximated linearly and the OPF formulations result  
 511 in convex optimisation problems. We have formulated a decentralised TSO-DSO co-  
 512 ordination scheme based on an iterative approach where no sensitive information is  
 513 exchanged that achieves a near optimal solution. Next, we have analysed the interaction  
 514 of TSOs and DSOs and how conflicting their objectives are by approximating the Pareto  
 515 front of a multi-objective OPF problem where the entire system, i.e., transmission and  
 516 distribution systems, is modelled. Through numerical results we have demonstrated  
 517 that both coordination schemes result in (i) reduced operational costs for both TSOs and  
 518 DSOs; (ii) congestion relief; and (iii) increased use of distributed generation.

519 *In the two proposed schemes different entities are responsible for making a decision;*  
 520 *and diverse information is shared between them. In particular, in the centralised scheme*  
 521 *the TSO makes the decisions and has access to all information about the underlying*  
 522 *physical distribution systems as well as DG bidding. In the decentralised scheme, both*  
 523 *the DSO and TSO share the decision making process and the only information that the*  
 524 *TSO sends the DSO is the LMP at the PCC and the DSO to the TSO its net load. The two*  
 525 *proposed methods also differ in the total cost; level of DG integration; voltage levels and*  
 526 *level of congestion, as demonstrated in the numerical results' section. These affect the*  
 527 *"power quality" of the system. However, all variables, e.g., voltage levels, transmission*

528 line flows, are kept within the limits of acceptable for power quality purposes as defined  
529 by the constraints of the OPFs.

530 There are natural extensions of the work presented here. For instance, a distributed  
531 solution of the proposed centralised scheme is necessary so that system operators do not  
532 share sensitive information about their topology and generators bids. Moreover, a more  
533 detailed representation on the topology of the distribution system would provide more  
534 accurate results as well as incorporation of uncertainty in renewable based generation.  
535 We will report on these developments in future papers.

### 536 *Appendix .1 Nomenclature*

### 537 *Appendix .2 Decentralised Scheme Detailed Formulation*

538 In Section 3.1 in (26) we provide the compact formulation of the proposed de-  
539 centralised scheme which is a bi-level optimisation problem. We do so to ease the  
540 readability of the paper and demonstrate the proposed methodologies. To make the  
541 formulation more clear we present here its detailed representation. The functions  
542  $f_1, f_2, g_1, g_2, h_1,$  and  $h_2$  can be easily mapped to the functions below:

$$\begin{aligned}
& \min_{P_{G_i}(t), i \in \mathcal{I}, B_i(t), k \in \mathcal{K}} \sum_{i \in \mathcal{I}} \left( \sum_{i \in \mathcal{I}} c_i(t) + \pi \sum_{i \in \mathcal{L}} (\theta_n(t) - \theta_m(t))^2 \right) \Delta t \\
& \text{subject to} \quad f^m \leq f(t) = B_d A \theta(t) \leq f^M, t \in \mathcal{T}, \\
& \quad P_G^m \leq P_G(t) \leq P_G^M, t \in \mathcal{T}, \\
& \quad \sum_{i \in \mathcal{I}_k} P_{G_i}(t) - \sum_{i \in \mathcal{L}} B_{d,i} A \theta(t) = P_{\text{grid}}^d(t), k \in \mathcal{K}, t \in \mathcal{T}, d \in \mathcal{D} \\
& \quad \forall d \in \mathcal{D}, P_{\text{grid}}^d(t) \in \arg \min_{\substack{P_{PV_i}(t), P_{B_i}^{\text{ch}}(t), \\ P_{B_i}^{\text{dis}}(t), V_i(t), \\ P_{\text{grid}}^d(t)}} \sum_{i \in \mathcal{I}} \left( \lambda_{k_d}(t) P_{\text{grid}}^d(t) + \sum_{i \in \mathcal{N}_{PV}^d} B_{PV_i} P_{PV_i}(t) + \sum_{i \in \mathcal{N}_B^d} B_{B_i} (P_{B_i}^{\text{ch}}(t) + P_{B_i}^{\text{dis}}(t)) + \sum_{i \in \mathcal{N}} \alpha (V_i(t) - V_{\text{ref}})^2 \right) \Delta t \\
& \quad \text{subject to} \quad P_{PV_i}^{\text{min}} \leq P_{PV_i}(t) \leq P_{PV_i}^{\text{max}}, i \in \mathcal{N}_{PV}, t \in \mathcal{T}, \\
& \quad P_{B_i}^{\text{ch,min}} \leq P_{B_i}^{\text{ch}}(t) \leq P_{B_i}^{\text{ch,max}}, i \in \mathcal{N}_B, t \in \mathcal{T}, \\
& \quad P_{B_i}^{\text{dis,min}} \leq P_{B_i}^{\text{dis}}(t) \leq P_{B_i}^{\text{dis,max}}, i \in \mathcal{N}_B, t \in \mathcal{T}, \\
& \quad V_i^{\text{min}} \leq V_i(t) \leq V_i^{\text{max}}, i \in \mathcal{N}, t \in \mathcal{T}, \\
& \quad P_{\text{grid}}^{\text{d,min}} \leq P_{\text{grid}}^d(t) \leq \sum_{i \in \mathcal{I}_k} P_{G_i}(t), t \in \mathcal{T}, \\
& \quad E_{\text{min},i} \leq \sum_{i \in \mathcal{I}} \left( \eta_{\text{ch},i} P_{B_i}^{\text{ch}}(t) - \frac{1}{\eta_{\text{dis},i}} P_{B_i}^{\text{dis}}(t) \right) \Delta t + E_{0,i} \leq E_{\text{max},i}, \forall i \in \mathcal{N}_B, t \in \mathcal{T}, \\
& \quad V(t) = R p(t) + X q(t) - M^{-1} m_0, t \in \mathcal{T}, \\
& \quad p_i(t) = P_{PV_i}(t) + P_{B_i}^{\text{dis}}(t) - P_{B_i}^{\text{ch}}(t) - P_{\text{load},i}(t), \forall i \in \mathcal{N}_{PV} \cap \mathcal{N}_B, t \in \mathcal{T}, \\
& \quad p_i(t) = P_{PV_i}(t) - P_{\text{load},i}(t), \forall i \in \mathcal{N}_{PV} \setminus \mathcal{N}_B, t \in \mathcal{T}, \\
& \quad p_i(t) = P_{B_i}^{\text{dis}}(t) - P_{B_i}^{\text{ch}}(t) - P_{\text{load},i}(t), \forall i \in \mathcal{N}_B \setminus \mathcal{N}_{PV}, t \in \mathcal{T}, \\
& \quad p_i(t) = -P_{\text{load},i}(t), \forall i \in \mathcal{N} \setminus \mathcal{N}_{PV} \cap \mathcal{N}_B, t \in \mathcal{T}, \\
& \quad q_i(t) = -Q_{\text{load},i}(t), \forall i \in \mathcal{N}, t \in \mathcal{T},
\end{aligned}$$

(A1)

543 where the objective of the upper level problem is the TSO cost minimisation and angle  
544 deviation; its constraints refer to power flow and generator limits and power balance.  
545 The lower level optimisation problem has as an objective the DSO cost and voltage  
546 regulation cost minimisation; its constraints refer to voltage, power, energy storage  
547 limits; and power balance. More details about the objective and constraints may be  
548 found in Section 2.

### 549 *Appendix .3 Centralised Scheme Detailed Formulation*

550 In Section 3.2 in (28) we provide the compact formulation of the proposed cen-  
551 tralised scheme to determine the Pareto front of the TSOs, DSOs objectives. To make  
552 the formulation more clear we present here its detailed representation. The functions  
553  $f_1, f_2, g_1, g_2, h_1,$  and  $h_2$  can be easily mapped to the functions below.

$$\begin{aligned}
& \min_{\substack{P_G(t), j \in \mathcal{J}, \\ \theta_n(t), k \in \mathcal{K}, \\ P_{PV_i}(t), P_{B_i}^{ch}(t), \\ P_{B_i}^{dis}(t), V_i(t)}}} \sum_{t \in \mathcal{T}} \left( w_1 \left( \sum_{i \in \mathcal{J}} c_i(t) + \pi \sum_{\ell=(m,n) \in \mathcal{L}} (\theta_n(t) - \theta_m(t))^2 \right) + w_2 \sum_{d \in \mathcal{D}} \left( \sum_{i \in \mathcal{N}_{PV}^d} B_{PV_i} P_{PV_i}(t) + \sum_{i \in \mathcal{N}_B^d} B_{B_i} (P_{B_i}^{ch}(t) + P_{B_i}^{dis}(t)) + \sum_{i \in \mathcal{N}} \alpha (V_i(t) - V_{ref})^2 \right) \right) \Delta t \\
& \text{subject to } f^m \leq f(t) = B_d A \theta(t) \leq f^M, \\
& P_G^m \leq P_G(t) \leq P_G^M, \\
& \sum_{i \in \mathcal{N}_d} P_G(t) - \sum_{i \in \mathcal{L}} B_{d_i} A \theta(t) = p_i^d(t), k \in \mathcal{K}, d \in \mathcal{D}, t \in \mathcal{T}, \\
& P_{PV_i}^{min} \leq P_{PV_i}(t) \leq P_{PV_i}^{max}, i \in \mathcal{N}_{PV}, t \in \mathcal{T}, d \in \mathcal{D}, \\
& P_{B_i}^{ch, min} \leq P_{B_i}^{ch}(t) \leq P_{B_i}^{ch, max}, i \in \mathcal{N}_B, t \in \mathcal{T}, d \in \mathcal{D}, \\
& P_{B_i}^{dis, min} \leq P_{B_i}^{dis}(t) \leq P_{B_i}^{dis, max}, i \in \mathcal{N}_B, t \in \mathcal{T}, d \in \mathcal{D}, \\
& V_i^{min} \leq V_i(t) \leq V_i^{max}, i \in \mathcal{N}, t \in \mathcal{T}, d \in \mathcal{D}, \\
& E_{min, i} \leq \sum_{t \in \mathcal{T}} \left( \eta_{ch, i} P_{B_i}^{ch}(t) - \frac{1}{\eta_{dis, i}} P_{B_i}^{dis}(t) \right) \Delta t + E_{0, i} \leq E_{max, i}, \forall i \in \mathcal{N}_B, t \in \mathcal{T}, d \in \mathcal{D}, \\
& V(t) = R p^d(t) + X q^d(t) - M^{-1} m_0, t \in \mathcal{T}, d \in \mathcal{D} \\
& p_i^d(t) = P_{PV_i}(t) + P_{B_i}^{dis}(t) - P_{B_i}^{ch}(t) - P_{load, i}(t), \forall i \in \mathcal{N}_{PV} \cap \mathcal{N}_B, t \in \mathcal{T}, d \in \mathcal{D}, \\
& p_i^d(t) = P_{PV_i}(t) - P_{load, i}(t), \forall i \in \mathcal{N}_{PV} \setminus \mathcal{N}_B, t \in \mathcal{T}, d \in \mathcal{D}, \\
& p_i^d(t) = P_{B_i}^{dis}(t) - P_{B_i}^{ch}(t) - P_{load, i}(t), \forall i \in \mathcal{N}_B \setminus \mathcal{N}_{PV}, t \in \mathcal{T}, d \in \mathcal{D}, \\
& p_i^d(t) = -P_{load, i}(t), \forall i \in \mathcal{N} \setminus \mathcal{N}_{PV} \cap \mathcal{N}_B, t \in \mathcal{T}, d \in \mathcal{D}, \\
& q_i^d(t) = -Q_{load, i}(t), \forall i \in \mathcal{N}, t \in \mathcal{T}, d \in \mathcal{D},
\end{aligned} \tag{A2}$$

554 where the objective of the centralised optimisation is the TSO cost, angle deviation, the  
555 DG cost and voltage regulation cost minimisation; its constraints refer to power flow  
556 and generator limits and power balance. The power balance in this case is modified to  
557 directly incorporate the real power injection/withdrawal at the PCC of each DSO. More  
558 details about the objective and constraints may be found in Section 2.

## References

- Gerard, H.; Rivero Puente, E.L.; Six, D. Coordination between transmission and distribution system operators in the electricity sector: A conceptual framework. *Utilities Policy* **2018**, *50*, 40–48. doi:<https://doi.org/10.1016/j.jup.2017.09.011>.
- Caramanis, M.C.; Goldis, E.; Ruiz, P.A.; Rudkevich, A. Power market reform in the presence of flexible schedulable distributed loads. New bid rules, equilibrium and tractability issues. 2012 50th Annual Allerton Conference on Communication, Control, and Computing (Allerton), 2012, pp. 1089–1096. doi:10.1109/Allerton.2012.6483339.
- Najibi, F.; Apostolopoulou, D.; Alonso, E. Enhanced performance Gaussian process regression for probabilistic short-term solar output forecast. *International Journal of Electrical Power & Energy Systems* **2021**, *130*, 106916.
- Najibi, F.; Alonso, E.; Apostolopoulou, D. Optimal Dispatch of Pumped Storage Hydro Cascade under Uncertainty. 2018 UKACC 12th International Conference on Control (CONTROL). IEEE, 2018, pp. 187–192.
- Kärkkäinen, S.; others. Integration of demand-side management, distributed generation, renewable energy sources and energy storages. *Report Task XVII Integration of Demand-Side management, Distributed Generation, Renewable Energy Sources and Energy Storages* **2008**, *1*, 77.
- de Jong, G.; Franz, O.; Hermans, P.; Lallemand, M. TSO-DSO data management report. *TSO-DSO Project Team, Tech. Rep* **2016**.
- Yuan, Z.; Hesamzadeh, M.R. Hierarchical coordination of TSO-DSO economic dispatch considering large-scale integration of distributed energy resources. *Applied Energy* **2017**, *195*, 600–615. doi:<https://doi.org/10.1016/j.apenergy.2017.03.042>.
- Hadush, S.Y.; Meeus, L. DSO-TSO cooperation issues and solutions for distribution grid congestion management. *Energy Policy* **2018**, *120*, 610–621.
- Birk, M.; Chaves-Ávila, J.P.; Gómez, T.; Tabors, R. TSO/DSO coordination in a context of distributed energy resource penetration. *Proc. EEIC*, 2016, pp. 2–3.
- Najibi, F.; Niknam, T.; Kavousi-Fard, A. Optimal stochastic management of renewable MG (micro-grids) considering electro-thermal model of PV (photovoltaic). *Energy* **2016**, *97*, 444–459. doi:<https://doi.org/10.1016/j.energy.2015.12.122>.
- Najibi, F.; Niknam, T. Stochastic scheduling of renewable micro-grids considering photovoltaic source uncertainties. *Energy Conversion and Management* **2015**, *98*, 484–499. doi:<https://doi.org/10.1016/j.enconman.2015.03.037>.
- Ashouri, A.; Sels, P.; Leclercq, G.; Devolder, O.; Geth, F.; D’hulst, R. Smart TSO-DSO interaction schemes, market architectures, and ICT solutions for the integration of ancillary services from demand-side management and distributed generation Network and market models, EU Report, Apr. 2017 **2017**.
- Givisiez, A.G.; Petrou, K.; Ochoa, L.F. A Review on TSO-DSO Coordination Models and Solution Techniques. *Electric Power Systems Research* **2020**, *189*, 106659. doi:<https://doi.org/10.1016/j.epsr.2020.106659>.
- Merino, J.; Gómez, I.; Turienzo, E.; Medina, C.; Cobelo, I.; Morch, A.; Saele, H.; Verpoorten, K.; Puente, E.; Häninnen, S.; others. Ancillary service provision by RES and DSM connected at distribution level in the future power system. *SmartNet project D* **2016**, *1*, 1.

15. Kristov, L.; De Martini, P.; Taft, J.D. A Tale of Two Visions: Designing a Decentralized Transactive Electric System. *IEEE Power and Energy Magazine* **2016**, *14*, 63–69. doi:10.1109/MPE.2016.2524964.
16. Savvopoulos, N.; Konstantinou, T.; Hatziargyriou, N. TSO-DSO coordination in decentralized ancillary services markets. 2019 International Conference on Smart Energy Systems and Technologies (SEST). IEEE, 2019, pp. 1–6.
17. Dempe, S.; Kalashnikov, V.; Pérez-Valdés, G.A.; Kalashnykova, N. Bilevel programming problems. *Energy Systems*. Springer, Berlin **2015**.
18. Papavasiliou, A. Analysis of distribution locational marginal prices. *IEEE Transactions on Smart Grid* **2017**, *9*, 4872–4882.
19. Sorin, E.; Bobo, L.; Pinson, P. Consensus-based approach to peer-to-peer electricity markets with product differentiation. *IEEE Transactions on Power Systems* **2018**, *34*, 994–1004.
20. Papavasiliou, A.; Mezghani, I. Coordination Schemes for the Integration of Transmission and Distribution System Operations. 2018 Power Systems Computation Conference (PSCC), 2018, pp. 1–7. doi:10.23919/PSCC.2018.8443022.
21. Saint-Pierre, A.; Mancarella, P. Active Distribution System Management: A Dual-Horizon Scheduling Framework for DSO/TSO Interface Under Uncertainty. *IEEE Transactions on Smart Grid* **2017**, *8*, 2186–2197. doi:10.1109/TSG.2016.2518084.
22. Huang, S.; Wu, Q.; Oren, S.S.; Li, R.; Z.Liu. Distribution Locational Marginal Pricing Through Quadratic Programming for Congestion Management in Distribution Networks. *IEEE Transactions on Power Systems* **2015**, *30*, 2170–2178. doi:10.1109/TPWRS.2014.2359977.
23. Rossi, M.; Migliavacca, G.; Viganò, G.; Siface, D.; Madina, C.; Gomez, I.; Kockar, I.; Morch, A. TSO-DSO coordination to acquire services from distribution grids: Simulations, cost-benefit analysis and regulatory conclusions from the SmartNet project. *Electric Power Systems Research* **2020**, *189*, 106700. doi:https://doi.org/10.1016/j.epsr.2020.106700.
24. Sun, J.; Tesfatsion, L.; Goldfarb, D.; Hogan, W.; Kirschen, D.; Liu, C.C.; McCalley, J.; Powell, M.J.D.; Price, J.; Salazar, H.; Wong, J.; Wu, T. DC Optimal Power Flow Formulation and Solution Using QuadProg \*. Technical report, 2010.
25. Zhu, H.; Liu, H.J. Fast local voltage control under the limited reactive power: optimality and stability analysis. *IEEE trans on power systems* **2016**, *31*, 3794 – 3803.
26. Franco, J.F.; Ochoa, L.F.; Romero, R. AC OPF for smart distribution networks: An efficient and robust quadratic approach. *IEEE Transactions on Smart Grid* **2017**, *9*, 4613–4623.
27. Montoya, O.D.; Gil-González, W.; Garces, A. Optimal Power Flow on DC Microgrids: A Quadratic Convex Approximation. *IEEE Transactions on Circuits and Systems II: Express Briefs* **2019**, *66*, 1018–1022. doi:10.1109/TCSII.2018.2871432.
28. Ochoa, L.N.; Pilo, F.; Keane, A.; Cuffe, P.; Pisano, G. Embracing an Adaptable, Flexible Posture: Ensuring That Future European Distribution Networks Are Ready for More Active Roles. *IEEE Power and Energy Magazine* **2016**, *14*, 16–28. doi:10.1109/MPE.2016.2579478.
29. Arnold, D.B.; Sankur, M.D.; Negrete-Pincetic, M.; Callaway, D.S. Model-Free Optimal Coordination of Distributed Energy Resources for Provisioning Transmission-Level Services. *IEEE Transactions on Power Systems* **2018**, *33*, 817–828. doi:10.1109/TPWRS.2017.2707405.
30. Vicente-Pastor, A.; Nieto-Martin, J.; Bunn, D.W.; Laur, A. Evaluation of Flexibility Markets for Retailer–DSO–TSO Coordination. *IEEE Transactions on Power Systems* **2019**, *34*, 2003–2012. doi:10.1109/TPWRS.2018.2880123.
31. Yang, R.; Hao, J.; Jiang, H.; Jin, X. Machine-Learning-Driven, Site-Specific Weather Forecasting for Grid-Interactive Efficient Buildings. Technical report, National Renewable Energy Lab.(NREL), Golden, CO (United States), 2020.
32. Krechel, T.; Sanchez, F.; Gonzalez-Longatt, F.; Chamorro, H.; Rueda, J.L. Chapter 11 - Transmission system-friendly microgrids: an option to provide ancillary services. In *Distributed Energy Resources in Microgrids*; Chauhan, R.K.; Chauhan, K., Eds.; Academic Press, 2019; pp. 291–321. doi:https://doi.org/10.1016/B978-0-12-817774-7.00011-9.
33. Association, E.; others. Open networks project: opening markets for network flexibility. *Energy Networks Association2017* **2017**.
34. Caramanis, M.; Ntakou, E.; Hogan, W.W.; Chakraborty, A.; Schoene, J. Co-Optimization of Power and Reserves in Dynamic T D Power Markets With Nondispatchable Renewable Generation and Distributed Energy Resources. *Proceedings of the IEEE* **2016**, *104*, 807–836. doi:10.1109/JPROC.2016.2520758.
35. D.B.West. *Introduction to Graph Theory*; Upper Saddle River: Orentice hall, 2001.
36. Morstyn, T.; Teytelboym, A.; Hepburn, C.; McCulloch, M.D. Integrating P2P Energy Trading with Probabilistic Distribution Locational Marginal Pricing. *IEEE Transactions on Smart Grid* **2019**, pp. 1–1. doi:10.1109/tsg.2019.2963238.
37. Bylling, H.C. Bilevel Optimization with Application in Energy. PhD thesis, University of Copenhagen, Faculty of Science, Department of Mathematical . . . , 2018.
38. von Stackelberg, H. *Market Structure and Equilibrium*; Springer, 1934.
39. Audet, C.; Hansen, P.; Jaumard, B.; Savard, G. Links between linear bilevel and mixed 0–1 programming problems. *Journal of optimization theory and applications* **1997**, *93*, 273–300.
40. Sinha, A.; Soun, T.; Deb, K. Using Karush-Kuhn-Tucker proximity measure for solving bilevel optimization problems. *Swarm and Evolutionary Computation* **2019**, *44*, 496–510. doi:https://doi.org/10.1016/j.swevo.2018.06.004.
41. Britzelmeier, A.; De Marchi, A.; Gerdtts, M., An Iterative Solution Approach for a Bi-level Optimization Problem for Congestion Avoidance on Road Networks. In *Numerical Methods for Optimal Control Problems*; Springer International Publishing: Cham, 2018; pp. 23–38. doi:10.1007/978-3-030-01959-4\_2.
42. J.Cohon. In *Multiobjective Programming and Planning*; Academic Press: New York, 1978.

43. Shan, S.; Wang, G.G. An Efficient Pareto Set Identification Approach for Multiobjective Optimization on Black-Box Functions. *Journal of Mechanical Design* **2004**, *127*, 866–874.
44. Vardani, B. Optimum Location of SVC in an IEEE 33 Bus Radial Distribution System Using Power Sensitivity Index. 2019 International Conference on Electrical, Electronics and Computer Engineering (UPCON), 2019, pp. 1–5. doi:10.1109/UPCON47278.2019.8980192.
45. Savier, J.S.; Das, D. Impact of Network Reconfiguration on Loss Allocation of Radial Distribution Systems. *IEEE Transactions on Power Delivery* **2007**, *22*, 2473–2480. doi:10.1109/TPWRD.2007.905370.
46. Baran, M.; Wu, F. Network reconfiguration in distribution systems for loss reduction and load balancing. *IEEE Transactions on Power Delivery* **1989**, *4*, 1401–1407. doi:10.1109/61.25627.
47. Sadiq, A.; Adamu, S.; Buhari, M. Optimal distributed generation planning in distribution networks: A comparison of transmission network models with FACTS. *Engineering Science and Technology, an International Journal* **2019**, *22*, 33–46. doi:https://doi.org/10.1016/j.jestch.2018.09.013.
48. Apostolopoulou, D.; Gross, G.; Güler, T. Optimized FTR Portfolio Construction Based on the Identification of Congested Network Elements. *IEEE Transactions on Power Systems* **2013**, *28*, 4968–4978. doi:10.1109/TPWRS.2013.2261097.